ARTICLE

OPEN ACCESS

Manipulation of a strigolactone transporter in tomato confers resistance to the parasitic weed broomrape

Xinwei Ban,[1,2] Li Qin,[1] Jijun Yan,[1] Jianxin Wu,[3] Qianjin Li,[1] Xiao Su,[4] Yanrong Hao,[1,2] Qingliang Hu,[1] Liquan Kou,[1] Zongyun Yan,[1] Peiyong Xin,[1] Yuqin Zhang,[2] Lemeng Dong,[5] Harro Bouwmeester,[5] Hong Yu,[1,6] Qinghui Yu,[7,8] Sanwen Huang,[9,10] Tao Lin,[4] Qi Xie,[1,2] Yuhang Chen,[1,2] Jinfang Chu,[1,2] Xia Cui,[3,11,*] Jiayang Li,[1,6,*] and Bing Wang[1,2,*]

*Correspondence: cuixia@zafu.edu.cn (X.C.); jyli@genetics.ac.cn (J.L.); bingwang@genetics.ac.cn (B.W.)

Received: December 29, 2024; Accepted: January 26, 2025; Published Online: March 3, 2025; https://doi.org/10.1016/j.xinn.2025.100815

GRAPHICAL ABSTRACT

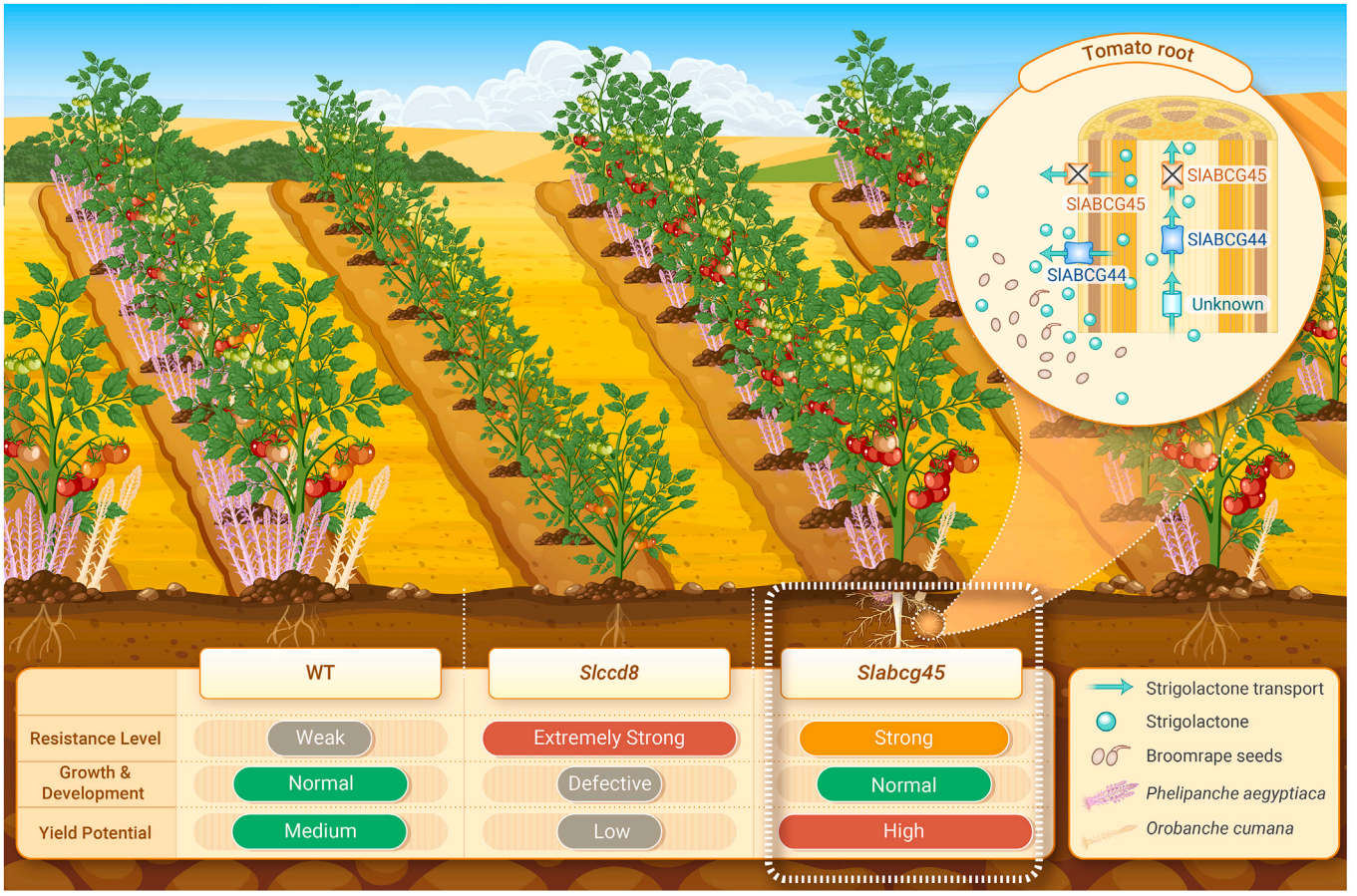

PUBLIC SUMMARY

- *SlABCG45* is closely associated with resistance to *Phelipanche aegyptiaca* in tomato.
- SlABCG45 and SlABCG44 mediate the exudation and upward transport of strigolactones in tomato.
- Genome editing of *SlABCG45* confers broad-spectrum parasite resistance without incurring a yield penalty.
- SlABCG45 is a promising breeding target for increasing crop yield in the fields infested with parasitic weeds.

OPEN ACCESS

ARTICLE

The Innovation

Manipulation of a strigolactone transporter in tomato confers resistance to the parasitic weed broomrape

Xinwei Ban,[1,2] Li Qin,[1] Jijun Yan,[1] Jianxin Wu,[3] Qianjin Li,[1] Xiao Su,[4] Yanrong Hao,[1,2] Qingliang Hu,[1] Liquan Kou,[1] Zongyun Yan,[1] Peiyong Xin,[1] Yuqin Zhang,[2] Lemeng Dong,[5] Harro Bouwmeester,[5] Hong Yu,[1,6] Qinghui Yu,[7,8] Sanwen Huang,[9,10] Tao Lin,[4] Qi Xie,[1,2] Yuhang Chen,[1,2] Jinfang Chu,[1,2] Xia Cui,[3,11,*] Jiayang Li,[1,6,*] and Bing Wang[1,2,*]

[1]State Key Laboratory of Seed Innovation and National Center for Plant Gene Research (Beijing), Institute of Genetics and Developmental Biology, Innovation Academy for Seed Design, Chinese Academy of Sciences, Beijing 100101, China

[2]College of Advanced Agricultural Sciences, University of Chinese Academy of Sciences, Beijing 100049, China

[3]State Key Laboratory of Vegetable Biobreeding, Sino-Dutch Joint Laboratory of Horticultural Genomics, Institute of Vegetables and Flowers, Chinese Academy of Agricultural Sciences, Beijing 100081, China

[4]Beijing Key Laboratory of Growth and Developmental Regulation for Protected Vegetable Crops, College of Horticulture, China Agricultural University, Beijing 100081, China

[5]Plant Hormone Biology Group, Swammerdam Institute for Life Sciences, University of Amsterdam, Amsterdam 1098 XH, the Netherlands

[6]Yazhouwan National Laboratory, Sanya 572024, China

[7]Key Laboratory of Genome Research and Genetic Improvement of Xinjiang Characteristic Fruits and Vegetables, Institute of Horticultural Crops, Xinjiang Academy of Agricultural Sciences, Urumqi 830000, China

[8]College of Life Science and Technology, Xinjiang University, Urumqi 830000, China

[9]National Key Laboratory of Tropical Crop Breeding, Shenzhen Branch, Guangdong Laboratory of Lingnan Modern Agriculture, Genome Analysis Laboratory of the Ministry of Agriculture and Rural Affairs, Agricultural Genomics Institute at Shenzhen, Chinese Academy of Agricultural Sciences, Shenzhen 518120, China

[10]National Key Laboratory of Tropical Crop Breeding, Chinese Academy of Tropical Agricultural Sciences, Haikou 571101, China

[11]Key Laboratory of Quality and Safety Control for Subtropical Fruit and Vegetable, Ministry of Agriculture and Rural Affairs, College of Horticulture Science, Zhejiang A&F University, Hangzhou 311300, China

*Correspondence: cuixia@zafu.edu.cn (X.C.); jyli@genetics.ac.cn (J.L.); bingwang@genetics.ac.cn (B.W.)

Received: December 29, 2024; Accepted: January 26, 2025; Published Online: March 3, 2025; https://doi.org/10.1016/j.xinn.2025.100815

Citation: Ban X., Qin L., Yan J., et al., (2025). Manipulation of a strigolactone transporter in tomato confers resistance to the parasitic weed broomrape. The Innovation **6(3)**, 100815.

Parasitic weeds of the Orobanchaceae family cause substantial economic losses and pose significant threats to global agriculture. However, management of such parasitism is challenging, and very few resistance genes have been cloned and characterized in depth. Here, we performed a genome-wide association study using 152 tomato accessions and identified *SlABCG45* as a key gene that mediates host resistance to *Phelipanche aegyptiaca* by affecting the level of strigolactones (SLs) in root exudates. SLs are synthesized and released by host plants and act as germination stimulants for parasitic weeds. We found that SlABCG45 and its close homolog SlABCG44 were membrane-localized SL transporters with essential roles in exudation of SLs to the rhizosphere, resistance to *Phelipanche* and *Orobanche*, and upward transport of SLs from roots to shoots. As a predominant environmental stimulant exacerbates parasitism, phosphorus deficiency dramatically induced *SlABCG45* expression and weakly induced *SlABCG44* expression via the transcription factors SlNSP1 and SlNSP2. Knockout of *SlABCG45* in tomato had little effect on yield traits in a broomrape-free field, but conferred increased resistance to different *Phelipanche* and *Orobanche* species, resulting in an ∼30% yield increase in a *Phelipanche*-infested field. Our findings reveal that targeting a single gene by genome editing can confer broad-spectrum parasite resistance in tomato, providing an effective strategy for the sustainable control of parasitic plants in agriculture.

INTRODUCTION

Obligate root parasites of the Orobanchaceae family, including *Striga*, *Orobanche*, and *Phelipanche* species, infest staple crops worldwide, leading to significant food insecurity and economic losses.[1–4] Parasitic plants have developed a unique heterotrophic lifestyle that enables them to absorb sugars, water, and nutrients from their hosts. The infected hosts become stunted and withered, resulting in huge yield losses.[5–7] Parasitic Orobanchaceae weeds are estimated to infest over 60 million hectares of farmland, causing billions of dollars in losses each year.[4] The yields of major cereal crops such as maize, sorghum, and millet are threatened by *Striga* worldwide, particularly in Africa.[4,8–10] In Europe, Asia, and the Middle East, broomrapes (*Orobanche* and *Phelipanche* spp.) are the main threats to economically important crops such as sunflower, tomato, tobacco, potato, and chickpea, causing marked reductions in yield, quality, and stress resistance.[2,11,12] For example, *Orobanche* infection of tomato, a major vegetable crop worldwide,[13] severely reduces fruit yield and quality, causing crop losses of up to 80% in heavily infested fields.[4,14]

The control of parasitic weeds in the field is challenging. It is time-consuming and laborious to eradicate such weeds from the field, and weed removal can also impair crop growth because of the tight belowground connections between parasites and hosts.[2] Herbicides against parasitic weeds are not sufficiently effective to support their large-scale application in agriculture.[15] Therefore, the breeding of elite crop varieties with high resistance to parasites is critical for parasitism control. To date, *Or1* to *Or7* have been reported as resistance loci or genes, among which *Or5* and *Or7* have been mapped to be involved in immunity responses.[12,15–17] A dominant gene from cowpea termed *RSG-301* encodes a typical nucleotide-binding domain and leucine-rich repeat containing protein that confers resistance to *Striga gesnerioides* race SG3.[18] In addition, the cowpea cultivar B301 exhibits resistance to *Striga gesnerioides* races SG4 and SG3 by developing a hypersensitive response, which is suppressed by a secreted effector protein from SG4z.[19] Thus, effector recognition and immunity responses of the host are important for parasite resistance. However, existing host-plant resistance is susceptible to being overcome by broomrape and witchweed populations, owing to the rapid evolution and considerable inter-population genetic variation of the parasites.[15,19,20] Thus, identification and utilization of genes that can confer durable resistance to *Orobanche* is important for the breeding of parasite-resistant crops.

Strigolactones (SLs) were discovered nearly 60 years ago as germination stimulants for parasitic plants of the Orobanchaceae family.[21–25] Intriguingly, host plants produce and release SLs to attract and form symbiotic interactions with arbuscular mycorrhizal (AM) fungi, thereby increasing their access to inorganic soil nutrients.[26] However, parasitic plants have evolved highly sensitive SL receptors to take advantage of the same signaling molecules for host recognition and seed germination.[27–30] As a class of carotenoid-derived plant hormones, SLs also function in various developmental processes, most prominently shoot branching or tillering in cereal crops.[31–38]

Crops with deficient, impaired, or altered SL production exhibit resistance to *Striga*, *Orobanche*, and/or *Phelipanche* species.[39–44] Mutation of *LOW GERMINATION STIMULATION 1* (*LGS1*) in sorghum resulted in a switch from 5-deoxystrigol (a dominant SL that triggers *Striga* germination) to orobanchol (an SL with low *Striga* germination activity), leading to enhanced *Striga* resistance and moderately reduced AM fungal colonization.[10] In maize, reducing the activity of SL biosynthesis enzymes altered SL composition and reduced *Striga* germination and infection, but it did not increase branch number.[8] Knockout of *SlCYP722C* in tomato led to reduced parasite germination without increasing branch number.[45] Recently, a wild pearl millet line showed reduced parasitism and improved AM fungi colonization, which are closely associated with the

deletion of an SL biosynthesis gene *PmCLAMT1b* and altered biosynthesis of orobanchol and pennilactone.[9]

Exudation of SLs from the roots to the rhizosphere is crucial for host-plant interactions with AM fungi and for parasitism by Orobanchaceae species. The ATP-binding cassette (ABC) transporter PDR1 from petunia is the first SL transporter identified in plants.[46] The *pdr1* mutant was deficient in SL exudation and showed impaired symbiotic interactions, lower *Phelipanche ramosa* germination rates, and hyper-branching phenotypes.[46,47] PDR1 homologs are also involved in SL transport in *Medicago truncatula* and tobacco.[48,49] In tomato, disruption of the two *PDR1* homologs *SlABCG44* and *SlABCG45* significantly reduced SL levels in root exudates and improved resistance to *Phelipanche aegyptiaca* infection in a pot assay.[50] However, further investigation is required to determine the endogenous substrates of SL transporters and the contribution of SL transporters to yield improvement in *Phelipanche*-infested fields.

Here, we performed a genome-wide association study (GWAS) on *Phelipanche*-resistance traits and identified SlABCG45 as an SL transporter with a central role in SL exudation and parasitism in tomato. Phosphorus (Pi) deficiency dramatically induced the expression of *SlABCG45* through the transcription factors SlNSP1 and SlNSP2. Knockout of *SlABCG45* reduced the upward transport of SLs without reducing fruit size or yield and significantly improved resistance to *Phelipanche* and *Orobanche*, thus elevating fruit yield in a *Phelipanche*-infested field.

MATERIALS AND METHODS

Plant materials and growth conditions

The 152 tomato accessions used in GWAS are listed in Table S1 and have been described previously.[51] The tomato variety of *S. pimpinellifolium* PI365967 has been described previously[52] and was used as the wild type for *Slabcg45-1*, *Slabcg45-2*, *Slabcg44-1*, *Slabcg44-2*, *Slabcg45-1/44-1*, *Slnsp1*, *Slnsp1/2*, and *Slccd8-2*. The tomato variety of *S. lycopersicum* cv. Moneymaker[52] was used as the wild type for *Slabcg45-3*, *Slabcg45-4*, *Slabcg44-3*, *Slabcg45-4/44-3*, and *Slccd8-1*. For RT-PCR, RNA sequencing, SL analysis, and upward $GR24^{4DO}$ transport assay, tomato seeds were surface-sterilized with 75% ethyl alcohol for 1 min and 30% sodium hypochlorite for 20 min, followed by five washes with sterile water. The seeds were then transferred to half-strength Murashige-Skoog (½ MS) medium containing 1.0% (w/v) sucrose and 0.7% agar at 25°C with a 16-h light/8-h dark photoperiod for 10 days. Then, the seedlings were transplanted to glass tubes and were grown hydroponically in half-strength Hoagland nutrient solution (pH 5.8) with 0 μM KH_2PO_4 (Pi deficient) or 200 μM KH_2PO_4 (Pi sufficient) in plant growth chamber (BPC600H, Fujian Jiupo Biotechnology, China) at 70% humidity with a 16-h light/8-h dark photoperiod at 25°C for several days. For mycorrhizal fungi inoculation, broomrape infection and field assays, tomato seeds were germinated on moistened filter paper at room temperature and then sown in 32-cell plastic flats in the greenhouse with 16-h light/8-h dark at 25°C. Seedlings with 3–4 true leaves were transplanted to pots.

Seeds of *P. aegyptiaca* were collected from infested fields in Xinjiang, China, and seeds of *O. cumana* race E and F were obtained from the laboratory of Prof. Jun Zhao at Inner Mongolia Agricultural University. *Arabidopsis thaliana* in Col-0 background was used for dual-luciferase reporter assays. *Arabidopsis* seeds were surface sterilized, vernalized at 4°C for 2–4 days, and germinated on ½ MS medium containing 1.0% (w/v) sucrose and 0.7% (w/v) agar. For preparation of protoplasts, seedlings were grown under a short-day photoperiod (8-h light, 16-h dark cycle) for 4 weeks.

Mycorrhizal fungi inoculation and broomrape infection

The 30-day-old tomato seedlings were transplanted into a mixture of vermiculite and sand (1:1, v/v) containing *Glomus intraradices* spores (~400 spores per plant) as described previously.[53,54] Proper amounts of water were supplied in the first 2 weeks for plant growth. Subsequently, adequate amounts of Hoagland solution without KH_2PO_4 were supplied to plants once a week until harvest.

For broomrape infection, seeds of *P. aegyptiaca* or *O. cumana* race E were preconditioned as described previously.[45] Around 20-day-old tomato seedings were transplanted into a mixture of vermiculite and soil (1:3, v/v) in 14 × 14 × 17-cm pots containing preconditioned broomrape seeds. Proper amounts of water and fertilizer were applied to the plants. Subsequently, the emerged, flowering and total numbers of *P. aegyptiaca* or *O. cumana* were counted.

GWAS

The 152 tomato accessions used for the GWAS were planted in a randomized block design in fields infested by *P. aegyptiaca* in Xinjiang, China. For each accession, we measured the number of emerged broomrapes in 5 plots with 16 tomato individuals per plot. To improve the accuracy of the field data, the tomato materials were planted in broomrape infested fields during the summer seasons of 2021 and 2022, and then in the greenhouse with pot systems containing broomrape seeds in 2023.

Reference genome sequences of SL2.50 and annotation files were downloaded from the Sol genomics network (https://solgenomics.net). Raw reads of whole-genome resequencing technology based on Illumina HiSeq 2000 platform for 152 tomato accessions were publicly available from community resources.[55] Clean reads were aligned to the reference genome using the bwa-mem method in BWA (version 0.7.17). A total of 4,427,482 single-nucleotide polymorphisms (SNPs) with an MAF > 0.05 and missing rate < 0.1 were used in the GWAS. Association analysis was performed with a mixed linear model implemented in the efficient mixed-model association expedited (EMMAX) software package. The BN (Balding-Nichols) kinship matrix was constructed using the filtered SNPs to estimate the proportion of randomly selected SNPs for each individual pair, with default parameters (emmax-kin -v -h -d 10). The first five principal components were included as fixed effects in the analysis. A significance threshold of 0.05 was applied for individual tests, and the effective number of independent SNPs (n) was determined using the GEC software (Genetic type I Error Calculator version 0.2; http://grass.cgs.hku.hk/gec/register.php). Manhattan plot displaying the GWAS results was generated by the R package "CMplot."

RNA isolation and real-time qPCR

RNA isolation, reverse transcription, and real-time qPCR were performed as described previously.[34,56] In brief, total RNA was extracted from each sample using TRIzol reagent (Invitrogen) according to the manufacturer's instruction. The quality of the total RNA was determined using a NanoDrop spectrophotometer (ThermoFisher). Reverse transcription was carried out with 2 μg of total RNA using Evo M-MLV RT Mix Kit (Agbio) according to the manufacturer's instruction. Real-time PCR experiments were conducted using gene-specific primers (Table S9) on the CFX 96 real-time PCR detection system (Bio-Rad) in a total volume of 10 μL system containing 5 μL of SsoFast EvaGreen supermix (Bio-Rad), 0.5 μL of both sense and antisense primers (each at 5 μM), 2 μL of diluted cDNA, and 2 μL of ddH_2O. Expression levels of target genes were normalized against that of tomato *UBIQUITIN* gene (Solyc01g056940). Error bars represent the SD from three independent experiments.

RNA sequencing analysis

Roots of 23-day-old tomato wild type (*S. pimpinellifolium* PI365967), *Slnsp1*, and *Slnsp1/2* were used for total RNA isolation. For each line, roots of 24 seedlings were collected for sampling. For each sample, 2 μg of total RNA was used to construct sequencing libraries according to the manufacturer's instruction. The libraries were sequenced at JMDNA Bio-Medical Technology (Shanghai) via a BGI DNBSEQ-T7, 150PE platform. Low-quality reads were removed with fastp (version 0.20.0), resulting in more than 6 Gigabytes of clean reads per library. The paired-end clean reads were then aligned by STAR (version 2.4.2a) to the tomato reference genome (SL2.5), which was downloaded from the Solanaceae (SOL) Genomics Network (http://solgenomics.net/). Fragment quantification was performed with FeatureCounts (version 1.5.0) in paired-end mode. The gene expression levels were calculated as fragments per kilobase of transcript per million fragments. Differential gene expression analyses were performed using the R (version 3.3.1) package DESeq (version 1.26.0) with the absolute value of log2 fold change >1 and $p < 0.05$.

Histochemical detection of GUS staining

Transgenic plants carrying the GUS reporter gene were immersed in 100 mM sodium phosphate buffer (pH 7.0) containing 0.1% Triton X-100, 1 mM 5-bromo-4-chloro-3-indolyl-β-d-glucuronic acid cyclohexylammonium salt (Sigma-Aldrich), 2 mM potassium ferricyanide, and 2 mM potassium ferrocyanide. Plants were subjected to vacuum treatment for 10 min and then incubated at 37°C for 16 h. The stained roots and shoots were fixed with 50% FAA (50% ethanol, 5% acetic acid, 5% formaldehyde), and embedded in 4% low-melting agarose (Amresco). Then, the fixed roots and shoots were sliced into 50- and 100-μm-thick transverse sections, respectively, using a microtome (Leica VT1200S). Light microscopy was performed with a stereomicroscope (Leica DMR).

Confocal laser scanning microscopy

Transgenic plants carrying the *pSlABCG45:NLS-YFP* or *pSlABCG44:NLS-YFP* gene were fixed with 50% FAA (50% ethanol, 5% acetic acid, 5% formaldehyde), and embedded in 4% low-melting agarose (Amresco). Then, the fixed roots were sliced into 150-μm-thick transverse sections using a microtome (Leica VT1200S). Root sections were imaged on a laser scanning confocal microscope (Zeiss LSM 980 inverted microscope), with an argon laser set at 514 nm for yellow fluorescent protein (YFP) and emission filters used at 508–570 nm. Image analysis was done with the ZEN lite software.

To observe the subcellular localization of SlABCG45-YFP and SlABCG44-YFP, transgenic roots were removed from the seedlings and stained with 8 μM FM4-64 on ice for 1 min, rinsed and mounted in water. Roots were imaged using a laser scanning confocal microscope (Zeiss LSM 980 inverted microscope), with an argon laser set at 514 nm for YFP and 510 nm for FM4-64 excitation. Emission filters used were 508–570 nm for YFP and 750 nm for FM4-64. Image analysis was done with ZEN lite software.

Efflux transport assay using *Xenopus* oocyte system and chemicals extraction from oocyte exudates

To detect the transport activity of SlABCG45 and SlABCG44, transport assay in *Xenopus* oocytes was carried as described.[57] The coding sequences (CDSs) of *SlABCG45* and *SlABCG44* were cloned into plasmid *pGHME2* for expression. Complementary RNA (cRNA) for all constructs were transcribed using T7 polymerase and the linear plasmids as templates. Oocyte sacs were digested in OR2 buffer (82.5 mM NaCl, 2.5 mM KCl, 1 mM $MgCl_2$, and 5 mM Hepes-Na [pH 7.5]) with 0.2 mg/mL collagenase (Sigma). By using a Drummond Nanoject II, the isolated oocytes were injected with 36 ng cRNA in 36 nL, and an equal volume of water injected as control. After incubated in ND96 buffer (96 mM NaCl, 1.8 mM $CaCl_2$, 1 mM $MgCl_2$, 2 mM KCl, and 5 mM Hepes-Na [pH 7.5]) for 40 h at 18°C, oocytes were further injected with 1.7 ng (23 nL) orobanchol, $GR24^{4DO}$, and $GR24^{ent-5DS}$, respectively. The oocytes injected with substrates were washed to remove cell surface residues and then incubated in 1.5 mL ND96 buffer for 2.5 h. After that, 1.2 mL of the incubation buffer was collected as oocyte exudates and was subjected to a purification procedure.

In brief, the oocyte exudates were loaded onto a pre-equilibrated Oasis HLB cartridge (Waters), which was subsequently washed with water to remove impurities. Then, orobanchol, $GR24^{4DO}$, and $GR24^{ent-5DS}$ were eluted with acetone, and the eluate was evaporated to dryness. The residue was re-dissolved in 50% acetonitrile in water for LC-MS/MS analysis.

Plant hydroponic cultivation conditions and SL extraction from root exudates

Seedlings of tomato (*S. pimpinellifolium* PI365967) were grown on ½ MS medium containing 1.0% (w/v) sucrose and 0.7% agar at 28°C with a 16-h light/8-h dark photoperiod for 10 days. Then, the seedlings were transferred to glass tubes and grown hydroponically in half-strength Hoagland nutrient solution without Pi for 12 days under the same conditions.

The SLs in root exudates were collected and purified as described previously.[34] After the collection of hydroponic culture medium, $GR24^{4DO}$ was added as an internal standard for the quantification of solanacol and orobanchol. Hydroponic culture medium was loaded onto a pre-equilibrated Oasis HLB cartridge (Waters). The SL-containing fractions were eluted with acetone, and the eluate was evaporated to dryness. The residue was re-dissolved in 50% acetonitrile in water for LC-MS/MS analysis.

LC-MS/MS analysis of SLs

SLs were analyzed using a UPLC-MS/MS system consisting of a UPLC system (Waters) equipped with a BEH C18 column (2.1 × 100 mm, 1.7 μm, Waters) and a QTRAP 5500 mass spectrometer (AB Sciex) equipped with an electrospray (ESI) source as described previously with minor modification.[58] The UPLC method was as follows: mobile phase A, 0.05% acetic acid in water; mobile phase B, 0.05% acetic acid in acetonitrile; column temperature, 30°C; flow rate, 0.3 mL/min; linear gradient: 0–15 min, 20% B to 80% B; 15–15.5 min, 80% B to 95% B; 15.5–16 min, 95% B; 16–17 min, 95% B to 20% B; 17–18 min, 20% B. SLs were detected in positive multiple reaction monitoring (MRM) mode. The ESI source parameters were set as follows: ion spray voltage, 4,500 V; desolvation temperature, 600°C; nebulizing gas 1, 50 psi; desolvation gas 2, 55 psi; and curtain gas, 40 psi. The selected MRM transition channels were 343.1 > 183.1 for solanacol, 347.1 > 233.1 for orobanchol, 334.1 > 216.1 for D_3-4DO, and 299.0 > 202.0 for GR24. Moreover, transition channels 343.1 > 97.1, 347.1 > 205.1, 334.1 > 234.1, and 299.0 > 185.0 were also monitored as a qualifier for solanacol, orobanchol, D_3-4DO, and GR24, respectively.

Germination assay of broomrape seeds

Seeds of *P. aegyptiaca*, and *O. cumana* races E and F were sterilized in a solution containing 30% bleach. After removing the solution, the seeds were washed 5 times with sterile water and conditioned for 7 days at 22°C on 8-mm glass fiber filter paper disks. Root exudate samples, $GR24^{4DO}$ (positive control) and water (negative control) were the applied to the preconditioned *Orobanche* seeds incubated at the same temperature. After 10 days, the germination rate was microscopically examined.

Luciferase activity assay in *Arabidopsis* protoplasts

Transformation of *Arabidopsis* leaf mesophyll protoplasts and measurement of transient transcriptional activation activity were performed as described previously.[59] The protoplasts were incubated overnight under dark environment. Protein was then isolated, and LUC activity was measured by the Dual-Luciferase Reporter Assay System (Promega) according to the manufacturer's instructions. The data are presented as the ratio of LUC/REN activity of three biological replicates.

Recombinant protein purification and electrophoretic mobility shift assays

The GST, SlNSP1-GST and SlNSP2-GST proteins were induced using 0.2 mM isopropyl β-d-1-thiogalactopyranoside at 16°C for 20 h in BL21 transetta cells (Transgene). Fusion proteins were purified using glutathione Sepharose 4 fast flow (GE Healthcare) and quantified by SDS-PAGE. Biotin 5'-end-labeled DNA probes were synthesized. Binding reaction samples containing 0.5 ng of biotin-labeled double-stranded DNAs, 0.2 μg of the recombinant protein GST, SlNSP1-GST, or SlNSP2-GST, and 1 μg of poly(dIdC) were incubated at room temperature for 20 min and subjected to electrophoresis on 6% (w/v) polyacrylamide gels with half-strength TBE buffer. Biotin-labeled DNA was detected using the Lightshift chemiluminescent electrophoretic mobility shift assays (EMSA) kit (Thermo Scientific).

Upward $GR24^{4DO}$ transport assay in tomato seedlings

The transport assay was conducted as reported previously.[46,47,60] In brief, the 14-day-old seedlings of wild type, *Slabcg45-1*, and *Slabcg44-1*were positioned vertically in a plastic pot (28 × 18 × 7 cm), with root orientated horizontally on moist asbestos covered with gauze. Droplets of 1.25% agar containing 3 ng $GR24^{4DO}$ were applied to roots at the position of 1 cm from the shoot-root junction. After 1.5 h, all roots were removed and the 3-cm shoot bases were collected and homogenized using liquid nitrogen. For each line, 10 plants were collected for SL quantification. Approximately 100 mg of homogenized tissue was extracted with methanol containing D_3-4DO as an internal standard for SL quantification. After extraction at 4°C overnight, the homogenates were centrifuged at 15,000 rpm for 15 min. The supernatants were collected and evaporated to dryness under nitrogen gas. The residue was dissolved in 20% ethyl acetate in *n*-hexane and applied onto a Sep-Pak Silica cartridge (Waters). The SL-containing fractions were eluted with ethyl acetate, and the eluate was evaporated to dryness. The residue was re-dissolved in 50% acetonitrile in water for LC-MS/MS analysis.

Phylogenetic tree

The phylogenetic tree was generated as described previously.[61] Protein sequences were aligned by Clustal W and the neighbor-joining tree was constructed in MEGA 7.0. The numbers represent bootstrap (1,000 replicates).

Plasmid construction and transgenic plant generation

To construct *35S:SlABCG45-YFP* and *35S:SlABCG44-YFP*, the CDSs of *SlABCG45* and *SlABCG44* were amplified with the primers SlABCG45-F-YFP, SlABCG45-R-YFP, SlABCG44-F-YFP, and SlABCG44-R-YFP and fused to the N terminus of *YFP-HA*.[62] To construct *pSlABCG45-GUS* and p*SlABCG44-GUS* plasmids, a 3,038-bp promoter of *SlABCG45* was amplified with primers proSlABCG45-GUS-F and proSlABCG45-GUS-R, and a 3,425-bp promoter of *SlABCG44* was amplified with primers pSlABCG44-GUS-F and pSlABCG44-GUS-R. The promoters were digested with *PstI*/*Bam*HI and *PstI*/*Xba*I for ligation into the binary vector *CP013*.[62] The *pSlABCG45:NLS-YFP* and *pSlABCG44:NLS-YFP* plasmids were generated by modifying the *pSlABCG45-GUS* and *pSlABCG44-GUS* plasmids, respectively. In brief, primers pSlABCG45-NLS-YFP-F/R and pSlABCG44-NLS-YFP-F/R were used to amplify the *NLS-YFP* CDS from the *pART27* vector.[63] The products were subsequently inserted into the linearized *pSlABCG45-GUS* and *pSlABCG44-GUS* plasmids digested by *Sma*I and *Sac*I. For CRISPR-Cas9 constructs, sgRNA binding sites were selected with CRISPR-P version 2.0 tool (http://cbi.hzau.edu.cn/CRISPR2/). The sgRNAX_U6_26t_SlU6p_sgRNAX fragments were amplified with primers containing sgRNAs and *Bsa*I recognition sites using a *pCBC_DT1T2_SlU6p* vector as the template, and then cloned into the vector *pTX041* at the *Bsa*I sites.[62] To generate *SlNSP1-GST*, *SlNSP2-GST*, *SlNSP1-FLAG*, and *SlNSP2-FLAG*, the CDSs of *SlNSP1* and *SlNSP2* were amplified and cloned into the *pCold-GST* and *pSCYCE-FLAG* vectors.[64] To generate the *proSlABCG45-LUC* and *proSlABCG44-LUC*, 2.0-kb promoters were amplified and cloned into *pGreen-0800-LUC*.[64] Plasmids were validated by sequencing and then transformed into the *Agrobacterium tumefaciens* strain AGL1. The transgenic plants were validated by PCR and sequencing. All primers used are listed in Table S9.

Accession numbers

The sequence data of the following genes (and their accession numbers) in this article can be found in the Sol Genomics Network (SGN): *SlABCG45* (Solyc08g067620); *SlABCG44* (Solyc08g067610); *SlD27* (Solyc09g065750); *SlCCD7* (Solyc01g090660); *SlCCD8*

(Solyc08g066650); *SlCYP722C* (Solyc02g084930), *SlMAX1* (Solyc08g062950), *SlCYP712G* (Solyc10g018150), *UBIQUITIN* (Solyc01g056940); *SlNSP1* (Solyc03g123400); *SlNSP2* (Solyc11g013150); *SlBCP1* (Solyc10g081520); *SlPT4* (Solyc06g051850); *SlPT5* (Solyc06g051860).

Quantification and statistical analysis

Data plotting and statistical tests were performed in GraphPad Prism 8. Statistical parameters, such as mean ± SD (standard deviation) and SEM (standard error), are indicated in the figure legends. In graphs, asterisks indicate statistical significance (*$p < 0.05$, **$p < 0.01$, ***$p < 0.001$; ns, not significant) according to two-tailed Student's t test and lowercase letters indicate statistical significance tested between multiple groups according to one-way ANOVA at $p < 0.05$.[65] The selection of sample size was based on extensive experience. All experiments involving measurements/quantifications, imaging and quantifications from images were repeated at least twice with similar results.

RESULTS

SlABCG45 is associated with *P. aegyptiaca* resistance in tomato

P. aegyptiaca is a holoparasite that infects tomato and causes severe yield losses in the field. To investigate the genomic basis for genetic variation in tomato *Phelipanche* resistance, we planted a panel of 152 diverse tomato accessions with high-quality genome resequencing data[51] in a field infested by *P. aegyptiaca*. These accessions include members of the red-fruit clade (*S. pimpinellifolium*, *S. lycopersicum* var. *cerasiforme*, and *S. lycopersicum*) from different geographic origins as well as a wild tomato accession[51] and showed various degrees of susceptibility to *P. aegyptiaca* (Figure 1A; Table S1). To minimize phenotypic inaccuracies and variability caused by uneven seed distribution of *P. aegyptiaca* in the soil, we monitored the emergence of broomrape plants in the infested fields over two seasons and also performed a pot assay in the greenhouse (Figures S1A and S1B; Table S1). We then performed GWAS using a mixed linear model and identified a major peak on chromosome 8, whose lead SNP exhibited a strong correlation with the average number of emerged *P. aegyptiaca* ($p = 4.66 \times 10^{-14}$) (Figures 1B and 1C). Linkage disequilibrium analysis of the peak region revealed that the strong association signals were concentrated in a 200-kb region that contained 21 genes (Figure 1D). Using a strict p value threshold ($p < 2.301387 \times 10^{-9}$), we identified 23 SNPs in this region, including one SNP in the intron of *Solyc08g067560*, 16 SNPs in the intron or coding region of *Solyc08g067620*, and additional SNPs in the intergenic regions (Figure S1C; Table S2). Given the close relationship between the degree of parasitism and the extent of Pi deficiency in the soil, we examined the transcript levels of the 21 candidate genes in response to Pi deficiency. *Solyc08g067620* exhibited the most substantial upregulation (over 40-fold), followed by *Solyc08g067580* (over 5-fold), *Solyc08g067700* (~3-fold), *Solyc08g067570* (over 2.5-fold), and *Solyc08g067610* (over 2-fold) (Figure 1E; Table S3). On the basis of these results, we considered *Solyc08g067620* to be a strong candidate gene associated with variation in *P. aegyptiaca* resistance of the tomato accessions.

SlABCG45 and SlABCG44 function as SL transporters

Solyc08g067620 encodes the full-size ABC transporter SlABCG45, which is a homolog of petunia PDR1.[46] The tomato genome also contains *Solyc08g067610*, which encodes SlABCG44, a close homolog with 91.54% protein identity to SlABCG45. To investigate the roles of *SlABCG45* and *SlABCG44*, we examined their tissue expression patterns and found that both were expressed mainly in root tissues, with *SlABCG44* showing higher expression levels than *SlABCG45* (Figure 2A). We then generated stable transgenic lines of *pSlABCG45:NLS–YFP*, *pSlABCG44:NLS–YFP*, *pABCG45:GUS*, and *pABCG44:GUS*. YFP and GUS signals showed that *SlABCG45* and *SlABCG44* were mainly expressed in the epidermal cells of tomato roots (Figures 2B and S2). The CDSs of *SlABCG45* and *SlABCG44* are ~4.5 kb in length and contain repetitive sequences and complex structures. It was difficult to amplify the entire CDSs and express intact SlABCG45 and SlABCG44 proteins, which contain 13 transmembrane domains. Great efforts were made to study the subcellular localization of SlABCG45 and SlABCG44, and stable transgenic lines expressing intact SlABCG45 or SlABCG44 fused with YFP were eventually generated in tomato. YFP signals indicated that both SlABCG45-YFP and SlABCG44-YFP were predominantly localized at the plasma membrane (Figure 2C).

We next investigated the transporter activities of intact SlABCG45 and SlABCG44 using the *Xenopus laevis* oocyte system, a well-established assay for the evaluation of protein transport functions.[66] Oocytes expressing SlABCG45 or SlABCG44 were injected with 1.7 ng orobanchol (a predominant endogenous SL in tomato[67,68]) for measurements of efflux transport. After incubation for 2.5 h, the orobanchol levels in the exudates were quantified using LC-MS/MS. The results showed that expression of SlABCG45 and SlABCG44 led to significantly higher orobanchol levels in the oocyte exudates compared with the control group (Figure 2D). The substrate specificity of the transporters was evaluated using GR24 compounds with different stereochemical features. Intriguingly, both SlABCG45 and SlABCG44 facilitated the export of $GR24^{4DO}$, an SL analog that specifically triggers SL signaling in plants,[33] but neither displayed export activity for $GR24^{ent-5DS}$, which functions as a karrikin analog[69] (Figure 2D). These findings strongly support the roles of SlABCG45 and SlABCG44 in the export of active SLs in *X. laevis* oocytes.

To evaluate the roles of SlABCG45 and SlABCG44 in SL exudation from tomato roots, we generated the knockout mutants *Slabcg45-1* and *Slabcg44-1* and the double mutant *Slabcg45-1/44-1* in the *S. pimpinellifolium* PI365967 (PP) background by genome editing (Figures S3A and S3B). The levels of orobanchol and solanacol, two predominant forms of active SLs in tomato,[67,68] were dramatically reduced in root exudates of *Slabcg45-1* and *Slabcg44-1* and almost undetectable in the *Slabcg45-1/44-1* double mutant (Figure 2E), indicating that SlABCG45 and SlABCG44 are essential for the exudation of endogenous SLs from the root to the rhizosphere. The germination rates of broomrape seeds were also dramatically reduced in Slabcg45-1, Slabcg44-1 and Slabcg45-1/44-1 mutants (Figure 2F). To investigate the responses of *SlABCG45* and *SlABCG44* to SLs, we performed $GR24^{4DO}$ treatment and generated knockout mutants of the SL biosynthesis gene *SlCCD8*. Upon $GR24^{4DO}$ treatment, expression levels of *SlABCG45* and *SlABCG44* increased more than 8.5- and 1.8-fold, respectively (Figure S3D). Accordingly, their expression levels were reduced in the *Slccd8-1* mutant, suggesting that these SL transporters undergo positive feedback regulation by their substrates (Figures S3C and S3E). The expression level of *SlABCG44* was also increased by ~20% in the *Slabcg45* mutant (Figure S3F). Because the expression of *SlABCG44* was almost 10 times higher than that of *SlABCG45* in the wild type, the increased expression of *SlABCG44* may partially compensate for the loss of *SlABCG45* function.

SlABCG45 and SlABCG44 partially mediate SL transport from roots to shoots

SLs have been known for almost 30 years as mobile signals that travel from the roots to the shoots, where they repress lateral bud elongation.[70–72] However, the transporters that facilitate upward SL transport and their roles in the regulation of shoot branching remain largely unknown. To investigate the functions of *SlABCG45* and *SlABCG44* in the upward transport of SLs, we examined branch development and assayed the transport activity of the SL analog $GR24^{4DO}$ in our *Slabcg* mutants. Compared with the wild type, the *Slabcg45* and *Slabcg44* mutants formed more branches, and the branch number of the *Slabcg45/44* double mutant was even higher (Figure 3A). Droplets containing 3 ng of $GR24^{4DO}$ were applied to the roots of mutant and wild-type seedlings in an upward SL transport assay, and $GR24^{4DO}$ contents were measured in the 3-cm shoot bases. $GR24^{4DO}$ levels in the shoot bases of *Slabcg45-2*, *Slabcg44-2*, and *Slabcg45-2/44-2* were reduced to 68%, 52%, and 43% of that in the wild type, demonstrating that root-to-shoot transport of $GR24^{4DO}$ was impaired by mutation of *SlABCG45* or *SlABCG44* (Figure 3B). These results indicate that *SlABCG45* and *SlABCG44* mediate SL transport from roots to shoots in tomato and that other unknown transporters may also participate in this upward transport.

Deficiency in SL biosynthesis has been reported to cause adverse developmental characteristics in rice, *Arabidopsis*, petunia, pea, tomato, maize, and sorghum.[8,39,41,42,44,73] We found that the *Slccd8* knockout mutant exhibited multiple phenotypes, including dwarfing, elongated axillary buds, and smaller fruits (Figures S4A and S4B). Interestingly, although the *Slabcg44* single mutant and the *Slabcg45/44* double mutant produced smaller fruits, the *Slabcg45* single mutant showed little change in fruit size (Figures S4C, S4D, and 3C). Importantly, when the *Slabcg45* mutant was grown in a broomrape-free field, the numbers and weights of green, red, and total fruits per plant were indistinguishable from those of the wild type (Figures 3D–3I), indicating that the *Slabcg45* mutation had little effect on yield traits of tomatoes grown in a field without broomrape infestation.

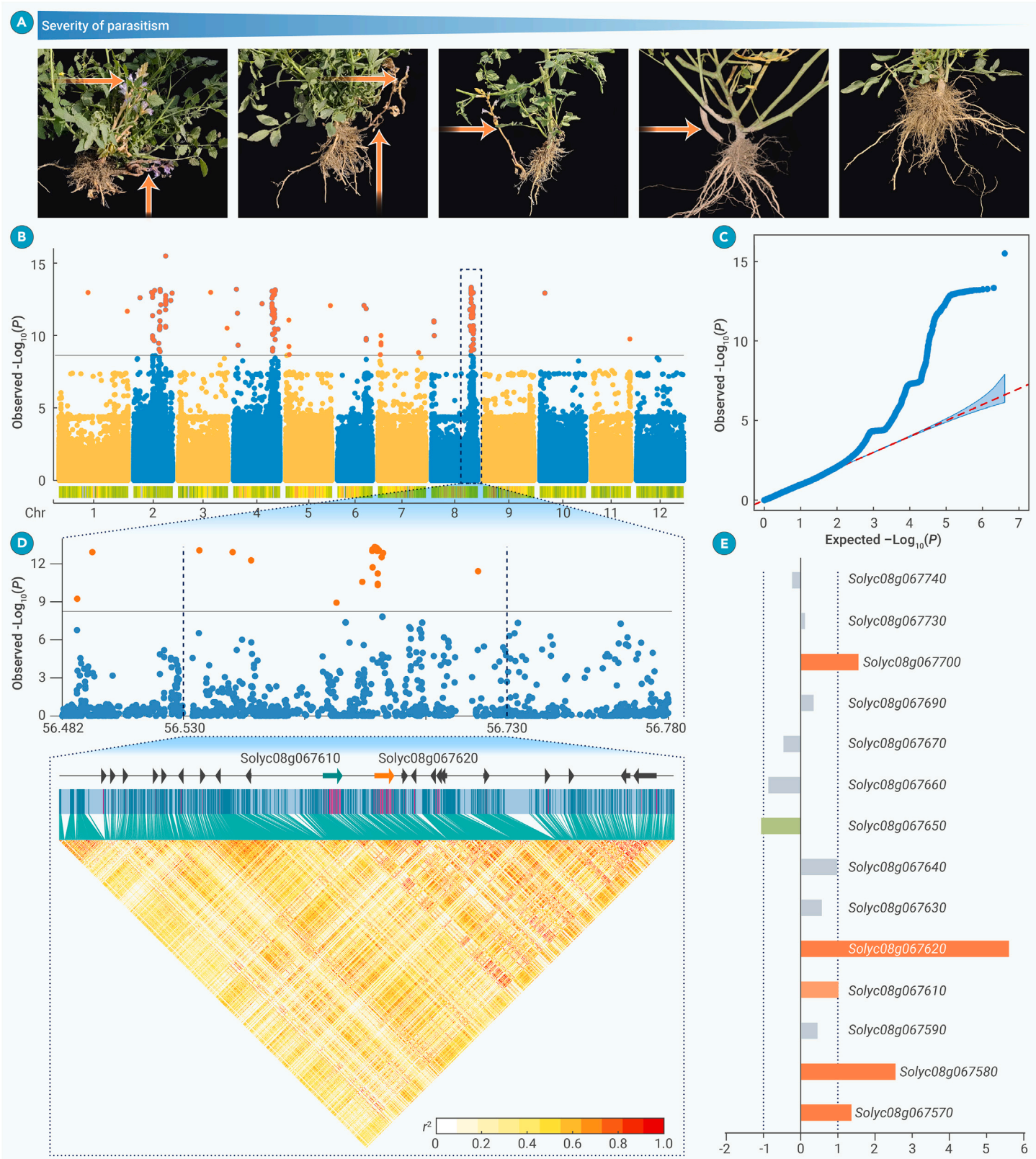

Figure 1. Identification of *Phelipanche* resistance loci through GWAS from 152 tomato accessions (A) Representative images of tomatoes with different *P. aegyptiaca* resistance (from left to right, TS-53, TS-299, TS-138, TS-220, TS-241). *P. aegyptiaca* was marked by arrows. (B) Manhattan plot of the GWAS for *P. aegyptiaca* resistance using a mixed linear model from the 152 accessions. (C) Quantile-quantile plot of *P. aegyptiaca* resistance. For the quantile-quantile plot, the $-\text{Log}_{10}$-transformed observed *p* values are plotted against the $-\text{Log}_{10}$-transformed expected *p* values. (D) Genome-wide Manhattan plot of the 56.482–56.780 Mb region on chromosome 8 and linkage disequilibrium plot for SNPs in the 56.53–56.73-Mb region. The black dashed lines indicate the candidate region for this peak. The red plots indicate the SNPs with *p* values above the threshold. A total of 21 candidate genes were identified within the 200-kb region, with *SlABCG45* (Soly08g067620) and *SlABCG44* (Soly08g067610) highlighted in orange and green, respectively. The color key (white to red) represents the linkage disequilibrium value (r^2). In (B) and (D), the threshold of observed $-\text{Log}_{10}(p)$ is 8.638, which is indicated by the gray line. *p* values were determined under the mixed linear model using the Wald test implemented in GEMMA. (E) Relative expression of candidate genes in response to phosphorus deficiency according to the RNA sequencing data. The black dashed lines indicate the 2-fold change (FC) of gene expression by phosphorus deficiency. Genes with Log_2 FC > 1 or Log2 FC < −1 are highlighted in orange and green, respectively. Genes with an FPKM value of zero were excluded from the graph. See also Figure S1 and Tables S1, S2, and S3.

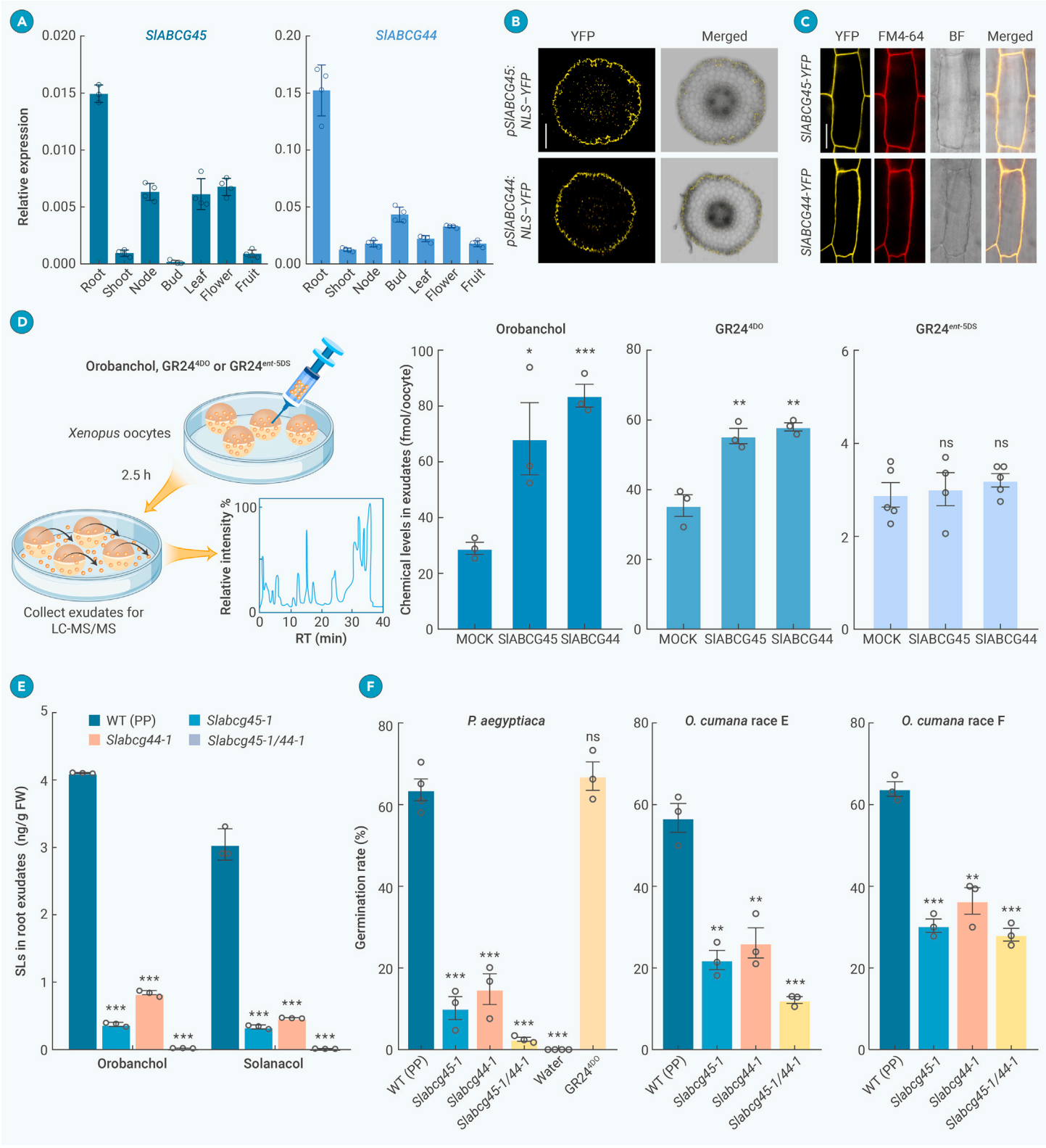

Figure 2. *SlABCG45* and *SlABCG44* encode membrane-localized SL transporters essential for broomrape germination (A) Transcript levels of *SlABCG45* and *SlABCG44* in various tissues. Data are mean ± SD, *n* = 3 biological replicates. (B) *pSlABCG45:NLS-YFP* and *pSlABCG44:NLS-YFP* signals (yellow) in tomato root sections. Scale bar, 100 μm. (C) Subcellular localization of SlABCG45-YFP and SlABCG44-YFP in tomato stable transgenic lines. The fluorescence was imaged in root epidermis. Roots were stained with the plasma membrane marker FM4-64. BF, bright field. Scale bar, 20 μm. (D) Efflux transport assay using the *Xenopus laevis* oocyte system. Oocytes were injected with cRNA encoding SlABCG45, SlABCG44, or water as a control. After 40 h, the oocytes were injected with 1.7 ng orobanchol (*n* = 3 biological replicates, each contains 3 oocytes), GR24^{4DO} (*n* = 3 biological replicates, each contains 3 oocytes), or GR24$^{ent-5DS}$ (*n* = 4 biological replicates, each contains 3 oocytes), respectively. After 2.5 h, the levels of the indicated compounds in the oocyte exudates were quantified using LC-MS/MS. Data are mean ± SEM. (E) Orobanchol and solanacol levels in root exudates of WT, *Slabcg45-1*, *Slabcg44-1*, and *Slabcg45-1/44-1*. Data are mean ± SEM, *n* = 3 biological replicates. (F) Germination assays of *P. aegyptiaca*, *O. cumana* race E, and *O. cumana* race F treated with root exudates of the indicated genotypes. GR24^{4DO} (0.3 μM) and water were used as positive and negative controls, respectively. Data are shown as mean ± SEM, *n* = 3 biological replicates. In (D–F), two-tailed Student's t test was used, $*p < 0.05$, $**p < 0.01$, $***p < 0.001$; ns, not significant. See also Figures S2 and S3.

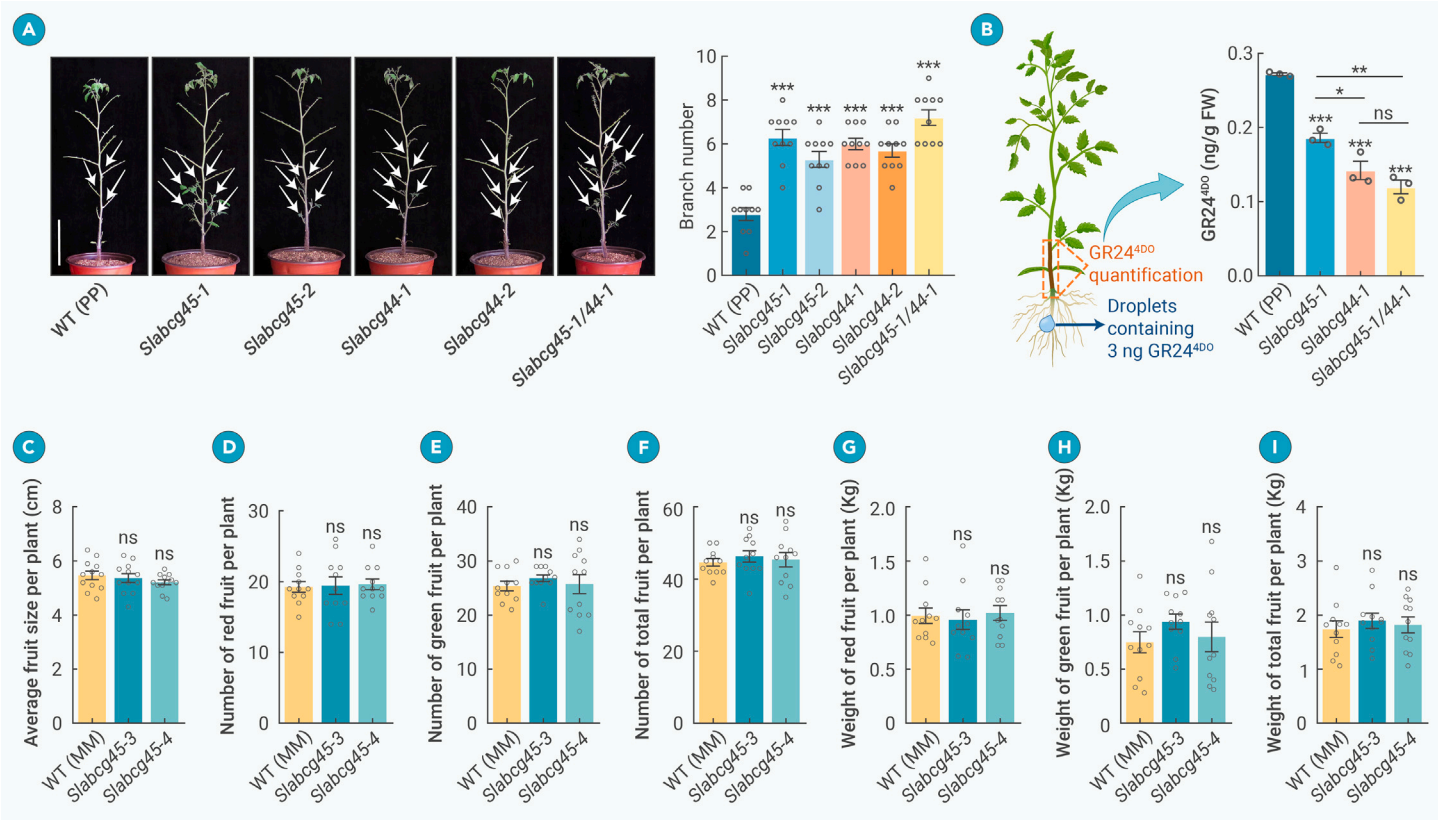

Figure 3. SlABCG45 is required for SL transport from roots to shoots but has little effect on tomato yield in broomrape-free field (A) Morphologies and branch numbers of WT, *Slabcg45-1*, *Slabcg45-2*, *Slabcg44-1*, *Slabcg44-2*, and *Slabcg45-1/44-1* mutants. Scale bar, 10 cm. Values are mean ± SEM, *n* = 10 plants. (B) Transport assay of $GR24^{4DO}$ in 14-day-old seedlings of WT, *Slabcg45-1*, *Slabcg44-1*, and *Slabcg45-1/44-1* mutants. Droplets of 1.25% agar containing 3 ng $GR24^{4DO}$ were applied to tomato roots. After 1.5 h, shoot bases of 3 cm were collected for quantification of $GR24^{4DO}$. Values are mean ± SEM, *n* = 3 biological replicates. (C) Average fruit size per plant of WT, *Slabcg45-3* and *Slabcg45-4*. Values are mean ± SEM, *n* = 12 plants. (D–I) Numbers of red (D), green (E), and total (F) fruits, and weights of red (G), green (H), and total (I) fruits per plant of WT and *Slabcg45* mutants in broomrape-free field. Values are mean ± SEM, *n* = 11 plants. In (A)–(I), two-tailed Student's t test was used, $*p < 0.05$, $**p < 0.01$, $***p < 0.001$; ns, not significant. See also Figure S4.

Pi deficiency induces transcription of *SlABCG45* and *SlABCG44* via SlNSP1 and SlNSP2

Orobanche and *Striga* parasitism are more severe on nutrient-depleted soils, especially those with Pi deficiency, which enhances SL biosynthesis and exudation.[74–77] However, the mechanism underlying SL exudation in response to Pi deficiency remains to be clarified. Because the expression of *SlABCG45* and *SlABCG44* was induced by Pi deficiency (Figure 1E), we searched for associated *cis*-elements in the *SlABCG45* and *SlABCG44* promoters and found multiple AATTT motifs that can be recognized by transcription factors from the GRAS family.[64,78] Our previous study revealed that Pi deficiency increases SL biosynthesis in rice roots mainly through the GRAS-type transcription factors OsNSP1 and OsNSP2.[64] We therefore investigated whether NSP1 and NSP2 were involved in the transcriptional induction of SL transporter genes in response to Pi starvation. Tomato *SlNSP1* was previously reported to be the homolog of *MtNSP1*,[79] and we found that *SlNSP1* and *SlNSP2* were homologs of *OsNSP1* and *OsNSP2*, respectively, and that their expression levels were significantly higher under Pi deficiency (Figures 4A and S5A; Table S4). We then investigated the transcriptional activity of SlNSP1 and SlNSP2 on the promoters of *SlABCG45* and *SlABCG44* in *Arabidopsis* protoplasts. SlNSP1-Flag and SlNSP2-Flag recombinant proteins showed relatively strong and weak transcriptional activation activities, respectively, on the *SlABCG45* promoter, but only SlNSP1-Flag exhibited significant transcriptional activation of the *SlABCG44* promoter (Figure 4B).

We next investigated whether these differences in transcriptional regulation were related to the binding activities of SlNSP1 and SlNSP2. EMSAs showed that addition of SlNSP1-GST led to a shifted band on the *SlABCG45* promoter. This band shift was strongly disturbed by competition from unlabeled probe in 50-fold excess but was unaffected by a similar quantity of mutant probe. Compared with SlNSP1-GST, recombinant SlNSP2-GST showed relatively weak binding signals, which were also competitively inhibited by a 50-fold excess of unlabeled probe (Figure 4C). Unlike the *SlABCG45* promoter, the *SlABCG44* promoter was bound by SlNSP1-GST rather than SlNSP2-GST (Figure 4D). These results indicate that SlNSP1 has relatively strong binding and transcriptional activation activities on the *SlABCG45* and *SlABCG44* promoters, whereas SlNSP2 exhibits weak or little effect. This mechanism differs from that by which OsNSP1 and OsNSP2 activate transcription of SL biosynthesis genes in rice.[64] In addition, the binding signals of SlNSP1-GST on the *SlABCG45* promoter were stronger than those on the *SlABCG44* promoter, consistent with the higher transcriptional activation of *SlABCG45* by SlNSP1 (Figures S5B and 4B).

Finally, we carried out a genetic study to evaluate the contributions of SlNSP1 and SlNSP2 to Pi starvation responses. We generated an *Slnsp1* knockout mutant and *Slnsp1/2* double mutant and performed transcriptome sequencing (RNA sequencing) of tomato seedlings grown under Pi-sufficient or Pi-deficient conditions for 14 days (Figures S5C and S5D). We identified 4,361, 2,612, and 2,645 differentially expressed genes between the two Pi conditions in the wild type, *Slnsp1*, and *Slnsp1/2*, respectively (Figure S5E; Tables S5, S6, and S7). All the known SL biosynthesis genes in tomato, including *SlD27*, *SlCCD7*, *SlCCD8*, *SlMAX1*, *SlCYP722C*, and *SlCYP712G*, were significantly upregulated by Pi deficiency in the wild type, but this upregulation was dramatically attenuated in the *Slnsp1* and *Slnsp1/2* mutants. Moreover, among all the *ABCG* genes in tomato,[80] *SlABCG45* showed the strongest induction under Pi deficiency in the wild type, and its induction was dramatically reduced in the *Slnsp1* and *Slnsp1/2* mutants. The expression of *SlABCG44* and *SlABCG56* was also weakly induced by Pi deficiency in a manner dependent on SlNSP1 and SlNSP2 (Figure S5F; Table S8). Reverse transcription qPCR (RT-qPCR) confirmed that *SlABCG45* expression increased over 35-fold under Pi deficiency, but this induction was reduced to 4.2- and 3.4-fold in *Slnsp1* and *Slnsp1/2*, respectively. Unlike that of *SlABCG45*, *SlABCG44* expression was induced ~1.6-fold under Pi deficiency in the wild type, but this induction was almost completely absent in the *Slnsp1* and *Slnsp1 Slnsp2* mutants (Figure 4E). Taken together, these results indicate that Pi deficiency alters the transcript levels of *SlABCG45* and *SlABCG44*, mainly through direct transcriptional regulation by SlNSP1 and SlNSP2, which

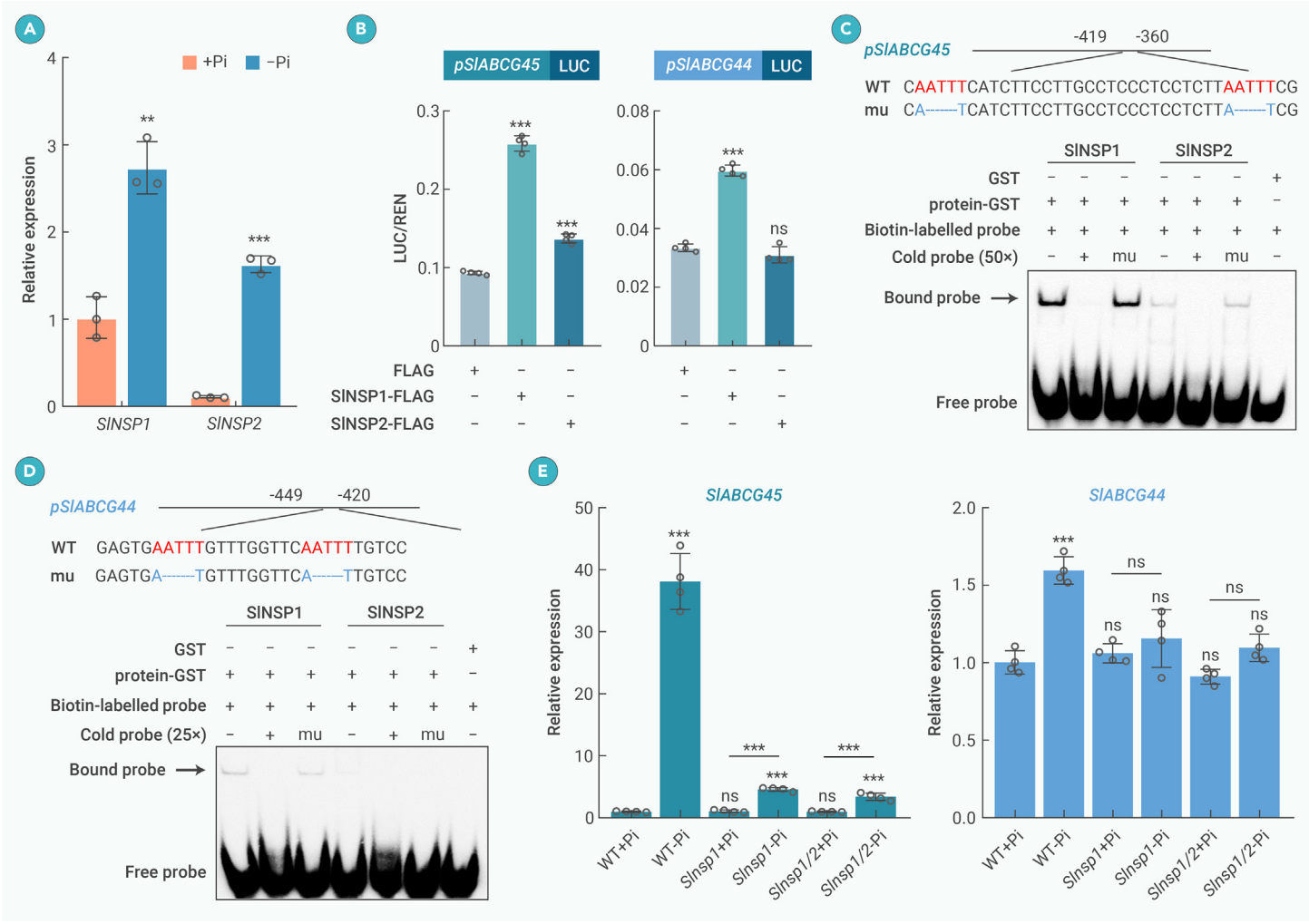

Figure 4. SlNSP1 and SlNSP2 are essential for transcriptional induction of *SlABCG45* by phosphorus deficiency (A) Transcript levels of *SlNSP1* and *SlNSP2* in wild-type seedlings grown in hydroponic medium with or without Pi for 14 days. Values are mean ± SD, $n = 3$ biological replicates. (B) Transcriptional activation of the SlNSP1-FlAG or SlNSP2-FlAG protein on the promoter of *SlABCG45* and *SlABCG44* in *Arabidopsis* protoplasts. Effectors were driven by the *35S* promoter, LUC was driven by the indicated promoters, and REN driven by the *35S* promoter was used as a reference. Values are mean ± SD, $n = 4$ biological replicates. (C) Binding activities of SlNSP1 and SlNSP2 to the *SlABCG45* promoter, assessed by EMSA. Probes were labeled with biotin, and 50-fold excess unlabeled probes were used for competition. (D) Binding activities of SlNSP1 and SlNSP2 to the *SlABCG44* promoter, assessed by EMSA. Probes were labeled with biotin, and 25-fold excess unlabeled probes were used for competition. (E) Transcript levels of *SlABCG45* and *SlABCG44* in seedlings of indicated plants grown in hydroponic medium with or without Pi for 14 days. Values are mean ± SD, $n = 4$ biological replicates. In (A), (B), and (E), two-tailed Student's t test was used, $^{**}p < 0.01$, $^{***}p < 0.001$; ns, not significant. See also Figure S5 and Tables S4, S5, S6, S7, and S8.

are essential for the induction of SL biosynthesis and exudation under Pi-limited conditions.

SlABCG45 mutation confers resistance to broomrapes at different inoculation densities

To investigate the effects of *SlABCG45* and *SlABCG44* disruption on host resistance to broomrape, we performed a *P. aegyptiaca* infection assay in pots in the greenhouse. Consistent with the SL levels in root exudates of the different mutants and their effects on seed germination, the number of emerged *P. aegyptiaca* plants was significantly lower in *Slabcg45-1*, *Slabcg44-1*, and *Slabcg45-1/44-1* mutants compared with the wild type (Figure 5A). The *SlABCG45* mutation had little effect on tomato yield under normal conditions but increased resistance to *P. aegyptiaca*, making it a promising target for balancing parasite resistance with tomato yield.

Broomrape seeds are unevenly distributed in the field environment, causing severe parasitism problems in localized areas.[4] To systematically evaluate the ability of *SlABCG45* mutation to enhance *P. aegyptiaca* resistance, we planted seedlings of the wild type and the *Slabcg45* mutant in soils with different inoculation densities of *P. aegyptiaca* seeds (Figure 5B). In pots containing 40 mg *P. aegyptiaca* seeds (representing normal density), the average number of emerged *P. aegyptiaca* that parasitized 2-month-old *Slabcg45-4* mutants was less than half that on the wild type. Notably, the average number of flowering *P. aegyptiaca* on *Slabcg45-4* plants was ~9.5% of that on wild-type plants, indicating that *SlABCG45* mutation delayed the onset of parasitism. When the seed densities were 80 and 120 mg/pot, there were again significantly fewer emerged and flowering *P. aegyptiaca* on the *Slabcg45* mutant, indicating that the effect of *SlABCG45* mutation on *P. aegyptiaca* control remains stable at higher inoculation densities.

Parasitic plant species show various levels of host specificity. Nonetheless, SLs act as common signaling molecules recognized by multiple parasites in the Orobanchaceae family. To determine whether knockout of *SlAGCG45* enhanced tomato resistance to parasitic species other than *P. aegyptiaca*, wild-type and *Slabcg45* seedlings were inoculated with seeds of *O. cumana* race E, which mainly parasitizes sunflower and causes substantial economic losses.[4] The total number of *O. cumana* on *Slabcg45-4* was ~40% of that on the wild type, and the number of flowering *O. cumana* was less than 15% of that on the wild type (Figure 5C). Collectively, these results demonstrate that knockout of *SlAGCG45* has the potential to confer durable and broad-spectrum resistance to various broomrape species in tomato.

Knockout of *SlABCG45* increased *Phelipanche* resistance and yield in an infested field

To evaluate the effect of *Slabcg45* on broomrape resistance and tomato yield under field conditions, we performed field experiments over two successive years in Xinjiang Province, a major tomato-producing region affected by

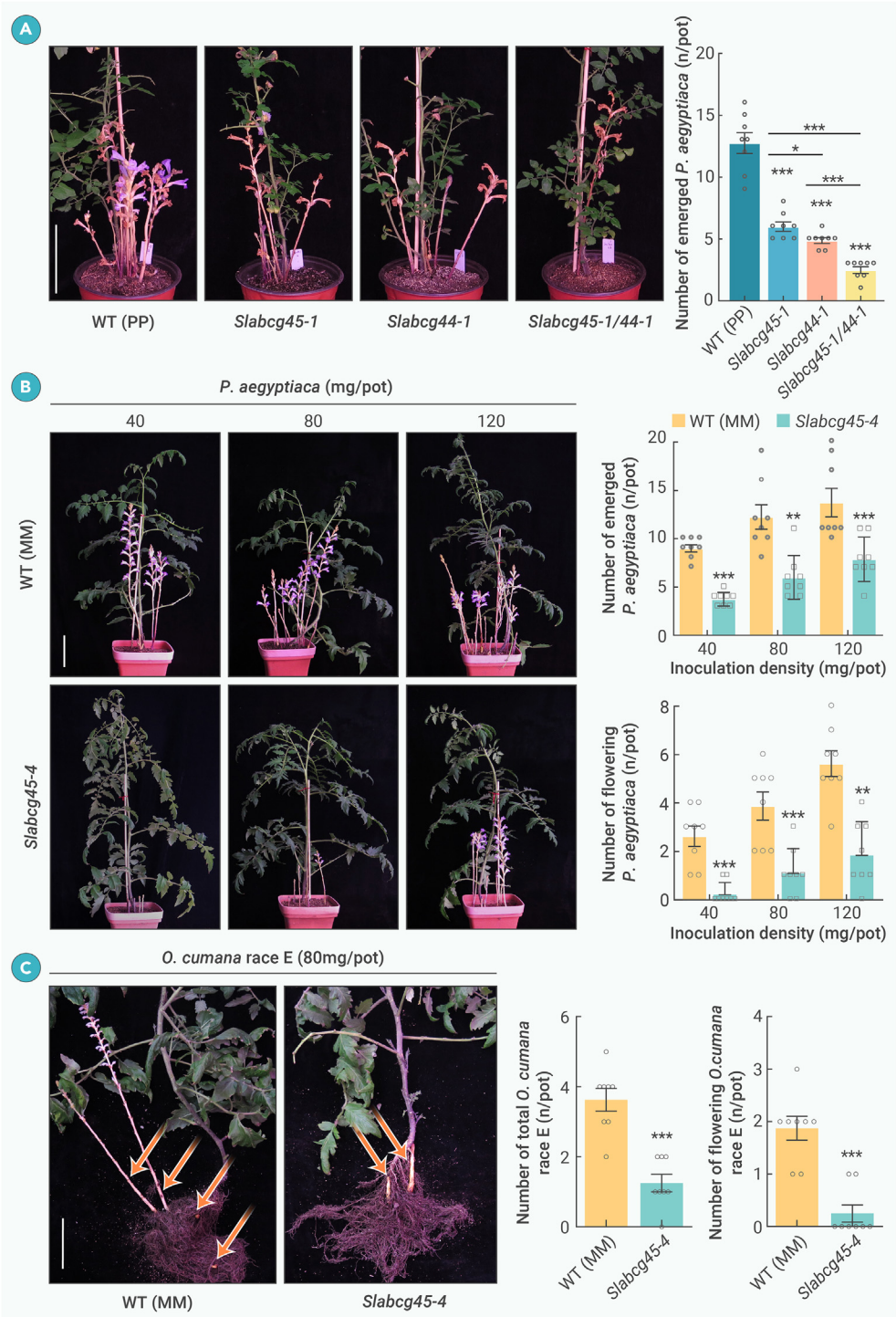

Figure 5. The *Slabcg45* mutant is resistant to broomrapes at different seed inoculation densities

(A) Parasitism of *P. aegyptiaca* on 3-month-old plants of WT, *Slabcg45-1*, *Slabcg44-1*, and *Slabcg45-1/44-1* mutants grown in the greenhouse. The inoculation density of *P. aegyptiaca* seeds was 40 mg/pot. Data are mean ± SEM, n = 8 plants. (B) Parasitism of *P. aegyptiaca* on 2-month-old WT and *Slabcg45-4* grown in the greenhouse under three parasite inoculation densities. The inoculation density of *P. aegyptiaca* seeds was 40, 80, or 120 mg per pot. Data are mean ± SEM, n = 8 plants. (C) Parasitism of *O. cumana* race E on 3-month-old plants of WT and *Slabcg45-4* grown in the greenhouse. The inoculation density of *O. cumana* seeds was 80 mg/pot. Data are mean ± SEM, n = 8 plants. Orange arrows indicate *O. cumana*. In (A–C), two-tailed Student's t test was used, $*p < 0.05$, $**p < 0.01$, $***p < 0.001$. Scale bars, 10 cm.

broomrapes in China. Wild-type plants and *Slabcg45*, *Slabcg44*, *Slabcg45/44*, and *Slccd8* mutants in the Moneymaker background were planted in four plots (Figure 6A). *P. aegyptiaca* number per plot was dramatically reduced in plots containing the *Slabcg45-3*, *Slabcg45-4*, and *Slabcg44-3* mutants compared with plots containing wild-type plants, and only a few *P. aegyptiaca* plants were observed in the *Slabcg45-4/44-3* and *Slccd8-1* plots in 2024 (Figures 6B and S6A). The fresh weight of *P. aegyptiaca* per plot was also dramatically reduced in *Slabcg45-3* and *Slabcg45-4* plots and was rather low in *Slccd8-1* plots (Figure 6C).

We also analyzed the effects of *SlABCG45*, *SlABCG44*, and *SlCCD8* on yield traits. Primary shoot heights of the wild type and the *Slabcg45*, *Slabcg44*, and *Slabcg45/44* mutants were similar, but *Slccd8* showed a severe dwarfing phenotype (Figures 6A, 6D, and S6B). Average fruit size and fruit weight per plant were comparable between the *Slabcg45* mutant and the wild type, but *Slccd8* had much smaller fruits (Figures 6E–6G). More importantly, the numbers of red, green, and total fruits per plant were significantly higher in *Slabcg45-3* and *Slabcg45-4* than in the wild type (Figures 6H–6K). Accordingly, the weights of red, green, and total fruits per plant were also higher in *Slabcg45-3* and *Slabcg45-4* (Figures 6L–6N). Similar trends were observed for the wild type and *Slabcg45* mutants in the 2023 field test, when *P. aegyptiaca* infestation was more severe (Figures S6I–S6P). Because of the negative effects of the *SlABCG44* mutation on fruit size (Figures S4C and S4D), although the numbers of red fruits and/or total fruits were higher in the *Slabcg44* and *Slabcg45/44* mutants, there was no significant increase in the weights of red, green, and total fruits in *Slabcg44* or *Slabcg45/44* mutants in 2024 (Figures S6C–S6H). In the *Slccd8* mutant, both fruit number and fruit weight were markedly reduced (Figures 6H–6N). In addition, after infection with AM fungi, the expression levels of AMF marker genes were much lower in the *Slccd8* mutant but only somewhat lower in the *Slabcg45* mutant, suggesting that symbiosis with AM fungi was stronger in *Slabcg45* than in *Slccd8* (Figure S7). Finally, to further evaluate the potential of *Slabcg45* to increase yield under infested conditions, we measured the total fruit weight in each plot. The yields of *Slabcg45-3* and *Slabcg45-4* were 33% and 36% higher, respectively, than those of the wild type, whereas the yield of *Slccd8* was 62% lower (Figure 6O). Taken together, these data demonstrate that knockout of *SlABCG45* increased resistance and improved yields in *Phelipanche*-infested fields.

DISCUSSION

SLs are intriguing carotenoid-derived plant compounds that act as rhizosphere signals to stimulate the germination of root-parasitic weeds and promote symbiosis with AM fungi. SLs also act as endogenous phytohormones to regulate various developmental processes and plant adaptation to nutrient availability. Crops with deficiencies in SL biosynthesis, such as *Slccd8*, exhibit resistance to broomrapes. However, the agricultural application of this strategy has been hampered by the accompanying undesirable traits, including dwarfing, excessive branch numbers, smaller and fewer fruit, and reduced fruit yield (Figure 7). Using GWAS and functional analyses, we identified SlABCG45 and SlABCG44 as

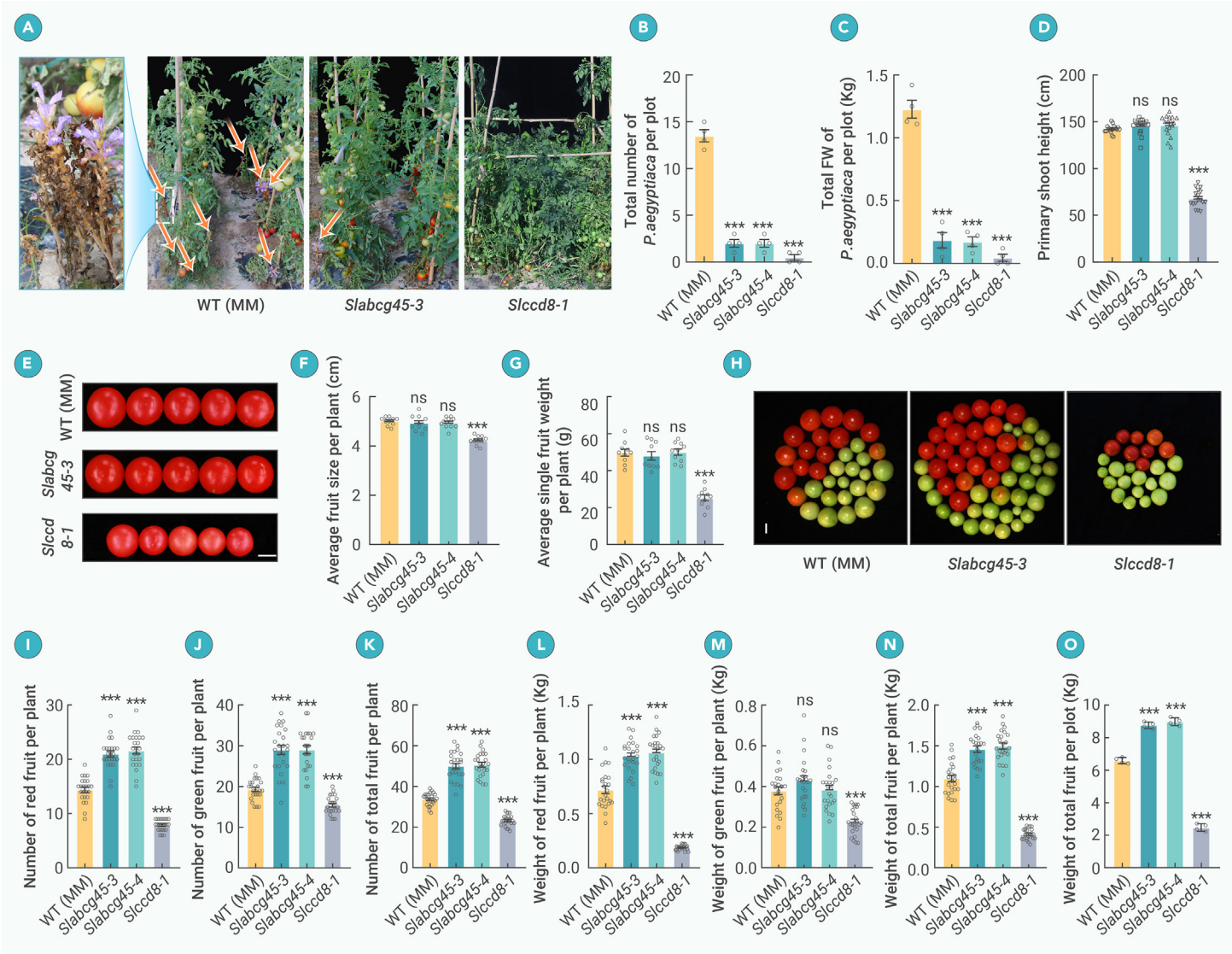

Figure 6. The *Slabcg45* mutants show elevated *P. aegyptiaca* resistance and fruit yield in an infested field (A) Representative photos of WT (Moneymaker [MM]), *Slabcg45-3*, and *Slccd8-1* in the *P. aegyptiaca*-infested field in 2024. Orange arrows indicate *P. aegyptiaca*. The magnified image in the upper left corner highlights the *P. aegyptiaca* obscured by tomato plants. Other obscured *P. aegyptiaca* weeds are not marked by arrows. (B and C) Total numbers (B) and fresh weights (C) of *P. aegyptiaca* parasitized on WT (MM), *Slabcg45-3*, *Slabcg45-4*, and *Slccd8-1* plants in each plot. Data are mean ± SEM, $n = 4$ plots. (D) Primary shoot height of WT (MM), *Slabcg45-3*, *Slabcg45-4*, and *Slccd8-1*. Data are mean ± SEM, $n = 17$ plants. (E–G) Representative photos, average fruit size and single fruit weight per plant of WT (MM), *Slabcg45-3*, *Slabcg45-4*, and *Slccd8-1*. Scale bar, 2.5 cm. Data are mean ± SEM, $n = 10$ plants. (H) Representative phenotypes of total fruits per plant of WT (MM), *Slabcg45-3* and *Slccd8-1*. Scale bar, 2.5 cm. (I–K) Numbers of red (I), green (J), and total (K) fruits per plant of the indicated genotypes. Data are mean ± SEM. $n = 24$ plants. (L–N) Weights of red (L), green (M), and total (N) fruits per plant of the indicated genotypes. Data are mean ± SEM. $n = 24$ plants. (O) Weights of total fruit of indicated genotypes in each plot. Data are mean ± SEM, $n = 4$ plots. Phenotypes were collected in Xinjiang, China, in 2024. In (B–D), (F and G), and (I–O), two-tailed Student's t test was used, $*p < 0.05$, $***p < 0.001$; ns, not significant. See also Figures S6 and S7.

important SL transporters that mediate SL secretion from the roots to the rhizosphere and are partially involved in SL transport from roots to shoots. Mutation of SlABCG45 or SlABCG44 significantly reduced SL exudation into the rhizosphere, conferring host resistance to notorious parasitic weeds. Notably, the *Slabcg45* mutant exhibited no obvious growth defects in a broomrape-free field and improved fruit yields associated with enhanced resistance in a broomrape-infested field (Figure 7). The expression of *SlABCG45*, rather than *SlABCG44*, was dramatically upregulated by Pi deficiency in a manner dependent on the direct binding and activation of SlNSP1 and SlNSP2. Given that parasitism is promoted in low-Pi environments, our findings suggest that *Slabcg45* has considerable potential for use in defense against broomrapes under different nutrient conditions.

SLs regulate plant development, facilitate symbiosis, and also act as germination stimulants for broomrape, a notorious parasite that absorbs nutrients from host plants and causes substantial yield losses in crops. In tomato, the wild-type plant produces and exudes SLs, causing parasitism when grown in the broomrape-infested field. Disruption of the SL biosynthesis gene *SlCCD8* eliminates germination of broomrape seeds due to SL deficiency in roots and rhizosphere, but leads to undesirable phenotypes such as dwarfing, more branches, reduced fruit size, and defective symbiosis. Mutation of the SL transporter *SlABCG45* significantly reduces the SL exudation to rhizosphere but retains a certain level of upward SL transport, allowing enhanced host resistance to broomrapes, moderately weakened symbiosis and largely unaffected shoot and fruit development.

SlABCG45 mutation confers durable parasite resistance in tomato

Perception of SLs produced by host plants is a precondition for successful root parasitism by members of the Orobanchaceae family. To adapt to the parasitic lifestyle, parasites have to endure high selection pressures associated with host co-evolution to achieve developmental flexibility.[81] This renders some commercial-resistant hybrids susceptible to *Orobanche* races with enhanced virulence.[20] As shown by transcriptome data and genome sequences of Orobanchaceae species, parasite evolution has proceeded in three phases: evolutionary gain of haustoria (phase I), loss of functions that are compensated by host resources (phase II), and specialization of parasitic relationships (phase III), during which some gene families expand while others contract.[82,83] It is noteworthy that a family of SL receptors has undergone significant expansion in several genomes of parasitic Orobanchaceae.[28–30] This is closely related to the fact that germination without a host root nearby would be risky, as germinated seeds cannot survive

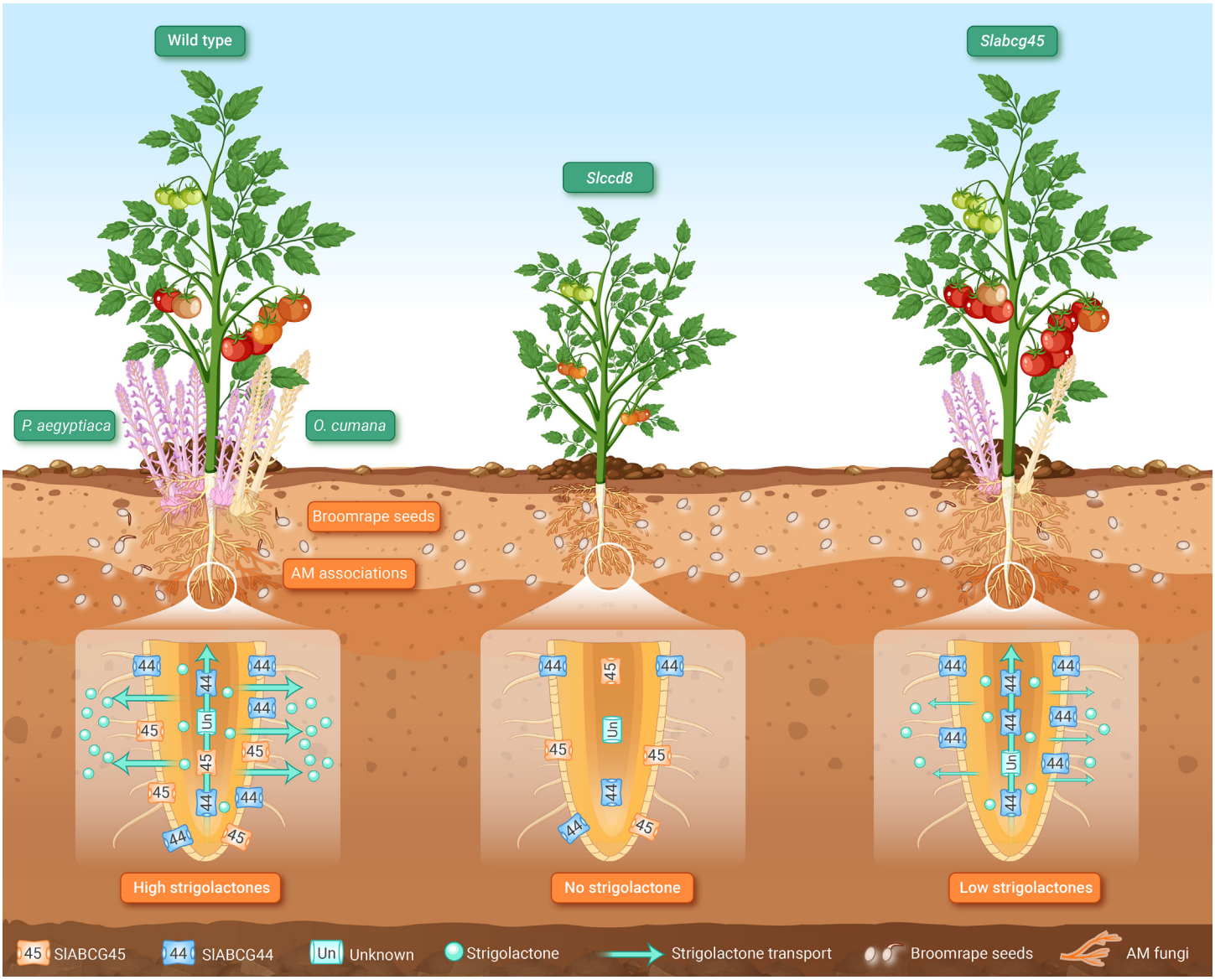

Figure 7. Proposed model for *SlABCG45*-mediated improvement of broomrape resistance and fruit yield in tomato As a result, the *Slabcg45* mutant exhibits significantly improved yield in the broomrape-infested field.

without rapidly connecting to a host. SLs, which are exuded in minute amounts and have unstable properties, form a concentration gradient in the rhizosphere that provides a positional cue to guide the parasites toward the host roots. Here, our findings reveal that rational manipulation of SL transporters shows great promise for the establishment of durable and broad resistance to *Phelipanche* and *Orobanche* in tomato.

Manipulation of *SlABCG45* promotes a balance between broomrape resistance and tomato yield

It is challenging to resolve the tradeoff between host broomrape resistance and high yields. Because complete disruption of SL biosynthesis has undesirable pleiotropic effects on host plants, as shown in the *Slccd8* knockout mutants (Figures 6, S4A, S4B, and S7), modulation of SL biosynthesis or transport to balance parasite resistance and tomato plant development is a more promising approach. Tomato *SlCCD8-RNAi* lines showed a 90% reduction in broomrape infestation but relatively mild changes in the AM symbiosis, apical dominance, and fruit yield.[84] Moreover, a partial loss-of-function allele of the SL biosynthesis gene *HIGH TILLERING AND DWARF 1/DWARF17* (*HTD1/D17*) in rice increased tiller number without compromising other agronomic traits, thereby improving grain yield.[85] Here, we demonstrated that mutation of *SlABCG45* in tomato significantly reduced *Orobanche* infection in both pot and field trials, with relatively modest effects on shoot architecture and the AM symbiosis. There are several potential reasons for the balance between resistance and growth observed in *Slabcg45*. First, *SlABCG45* expression responded strongly to phosphorus deficiency, an environmental signal that induces parasitism, SL biosynthesis, and exudation. The expression of *SlABCG44* was higher than that of *SlABCG45* under normal conditions but responded only weakly to phosphorus deficiency. SlABCG45 and SlABCG44 are close homologs and showed comparable transport activities in oocytes and upward SL transport assays. The expression of *SlABCG44* was increased in the *Slabcg45* mutant and may partially compensate for the lack of *SlABCG45* function, especially under normal growth conditions. Thus, SL exudation and parasitism were dramatically reduced in roots of the *Slabcg45* mutant without sacrificing fruit development and tomato yield. Second, analyses of upward SL transport suggested that *SlABCG45* and *SlABCG44* were only partially responsible for the long-distance transport of SLs (Figure 3B). Therefore, mutation of *SlABCG45* had a relatively weak effect on shoot architecture compared with mutation of *SlCCD8*. Moreover, recent studies have shown that orobanchol does not contribute significantly to the inhibition of shoot branching/tillering but does act as an important rhizosphere signal in rice.[86] Consistently, we found that the *Slabcg45* mutant had reduced orobanchol levels in its root exudates and showed relatively weak defects in shoot architecture. But the *SlABCG45* mutation caused relatively weak reduction in

the expression of AMF marker genes (Figure S7), perhaps because other SL compounds were still exuded to the rhizosphere. It would be interesting to determine whether other endogenous SLs serve as substrates for SlABCG45 and SlABCG44 and whether unknown SL transporters are also involved in exudation of SLs to the rhizosphere.

Tomato is the most economically important vegetable crop worldwide. However, parasitism can dramatically reduce the yield and quality of tomato fruits, and no commercial *Orobanche*-resistant tomato varieties or accessions are widely used in agricultural production. On the basis of these exciting findings, genome editing[87,88] could be used to generate knockout mutants of key SL transporters to achieve a balance between parasite resistance and tomato yield. This strategy could enable widespread application of precision breeding for *Orobanche*- and *Striga*-resistant crops in the near future.

CONCLUSION

We demonstrated that *SlABCG45* and its homolog *SlABCG44* regulate tomato resistance to *P. aegyptiaca*. We systematically characterized the roles of their encoded proteins in outward and upward transport of SLs and revealed a molecular network that modulates SL exudation in response to Pi deficiency. Manipulation of *SlABCG45* promoted a balance between *P. aegyptiaca* resistance and plant development, resulting in improved tomato yield in *P. aegyptiaca*-infested fields. These findings demonstrate that alteration of a single gene through genome editing can confer stable and broad-spectrum parasite resistance, providing an efficient breeding strategy for the control of parasitic weeds worldwide.

DATA AND CODE AVAILABILITY

The RNA-seq data have been deposited in the Gene Expression Omnibus (www.ncbi.nlm.nih.gov/geo/) under the accession number GEO: GSE284240. Materials and reagents are available from the corresponding authors upon reasonable request.

REFERENCES

1. Clarke, C.R., Timko, M.P. and Yoder, J.I. (2019). Molecular dialog between parasitic plants and their hosts. *Annu. Rev. Phytopathol.* **57**:279–299.
2. Mutuku, J.M., Cui, S. and Yoshida, S. (2021). Orobanchaceae parasite-host interactions. *New Phytol.* **230**:46–59.
3. Yoshida, S. and Shirasu, K. (2012). Plants that attack plants: molecular elucidation of plant parasitism. *Curr. Opin. Plant Biol.* **15**:708–713.
4. Parker, C. (2009). Observations on the current status of *Orobanche* and *Striga* problems worldwide. *Pest Manag. Sci.* **65**:453–459.
5. Kokla, A. and Melnyk, C.W. (2018). Developing a thief: Haustoria formation in parasitic plants. *Dev. Biol.* **442**:53–59.
6. Yoshida, S., Cui, S. and Ichihashi, Y. (2016). The Haustorium, a Specialized Invasive Organ in Parasitic Plants. *Annu. Rev. Plant Biol.* **67**:643–667.
7. Yoder, J.I. and Scholes, J.D. (2010). Host plant resistance to parasitic weeds; recent progress and bottlenecks. *Curr. Opin. Plant Biol.* **13**:478–484.
8. Li, C., Dong, L. and Durairaj, J. (2023). Maize resistance to witchweed through changes in strigolactone biosynthesis. *Science* **379**:94–99.
9. Kuijer, H.N.J., Wang, J.Y. and Bougouffa, S. (2024). Chromosome-scale pearl millet genomes reveal CLAMT1b as key determinant of strigolactone pattern and *Striga* susceptibility. *Nat. Commun.* **15**:6906.
10. Gobena, D., Shimels, M. and Rich, P.J. (2017). Mutation in sorghum *LOW GERMINATION STIMULANT 1* alters strigolactones and causes *Striga* resistance. *Proc. Natl. Acad. Sci. USA* **114**:4471–4476.
11. Bai, J., Wei, Q. and Shu, J. (2020). Exploration of resistance to *Phelipanche aegyptiaca* in tomato. *Pest Manag. Sci.* **76**:3806–3821.
12. Duriez, P., Vautrin, S. and Auriac, M.-C. (2019). A receptor-like kinase enhances sunflower resistance to *Orobanche cumana*. *Nat. Plants* **5**:1211–1215.
13. Tomato Genome Consortium (2012). The tomato genome sequence provides insights into fleshy fruit evolution. *Nature* **485**:635–641. DOI:https://doi.org/10.1038/nature11119.
14. Longo, A.M.G., Lo Monaco, A. and Mauromicale, G. (2010). The effect of *Phelipanche ramosa* infection on the quality of tomato fruit. *Weed Res.* **50**:58–66.
15. Fernández-Aparicio, M., Delavault, P. and Timko, M.P. (2020). Management of Infection by Parasitic Weeds: A Review. *Plants* **9**:1184.
16. Rodríguez-Ojeda, M.I., Pineda-Martos, R., Alonso, L.C. et al. (2013). A dominant avirulence gene in *orobanche cumana* triggers *r5* resistance in sunflower. *Weed Res.* **53**:322–327.
17. Tang, S., Heesacker, A. and Kishore, V.K. (2003). Genetic mapping of the Or5 gene for resistance to Orobanche race E in sunflower. *Crop Sci.* **43**:1021–1028.
18. Li, J. and Timko, M.P. (2009). Gene-for-Gene Resistance in *Striga* -Cowpea Associations. *Science* **325**:1094.
19. Su, C., Liu, H. and Wafula, E.K. (2020). SHR4z, a novel decoy effector from the haustorium of the parasitic weed *Striga gesnerioides*, suppresses host plant immunity. *New Phytol.* **226**:891–908.
20. Martín-Sanz, A., Malek, J. and Fernández-Martínez, J.M. (2016). Increased Virulence in Sunflower Broomrape (*Orobanche cumana* Wallr.) Populations from Southern Spain Is Associated with Greater Genetic Diversity. *Front. Plant Sci.* **7**:589.
21. Yokota, T., Sakai, H. and Okuno, K. (1998). Alectrol and orobanchol, germination stimulants for *Orobanche minor*, from its host red clover. *Phytochemistry* **49**:1967–1973.
22. Hauck, C., Müller, S. and Schildknecht, H. (1992). A Germination Stimulant for Parasitic Flowering Plants from *Sorghum bicolor*, a Genuine Host Plant. *J. Plant Physiol.* **139**:474–478.
23. Siame, B.A., Weerasuriya, Y. and Wood, K. (1993). Isolation of strigol, a germination stimulant for *Striga asiatica*, from host plants. *J. Agric. Food Chem.* **41**:1486–1491. DOI:https://doi.org/10.1021/jf00033a025.
24. Cook, C.E., Whichard, L.P. and Turner, B. (1966). Germination of Witchweed (*Striga lutea* Lour.): Isolation and Properties of a Potent Stimulant. *Science* **154**:1189–1190.
25. Müller, S., Hauck, C. and Schildknecht, H. (1992). Germination stimulants produced by *Vigna unguiculata Walp* cv Saunders Upright. *J. Plant Growth Regul.* **11**:77–84.
26. Chesterfield, R.J., Vickers, C.E. and Beveridge, C.A. (2020). Translation of Strigolactones from Plant Hormone to Agriculture: Achievements, Future Perspectives, and Challenges. *Trends Plant Sci.* **25**:1087–1106.
27. Takei, S., Uchiyama, Y. and Bürger, M. (2023). A Divergent Clade KAI2 Protein in the Root Parasitic Plant *Orobanche minor* Is a Highly Sensitive Strigolactone Receptor and Is Involved in the Perception of Sesquiterpene Lactones. *Plant Cell Physiol.* **64**:996–1007.
28. Toh, S., Holbrook-Smith, D. and Stogios, P.J. (2015). Structure-function analysis identifies highly sensitive strigolactone receptors in *Striga*. *Science* **350**:203–207.
29. Tsuchiya, Y., Yoshimura, M. and Sato, Y. (2015). Probing strigolactone receptors in Striga hermonthica with fluorescence. *Science* **349**:864–868.
30. Conn, C.E., Bythell-Douglas, R. and Neumann, D. (2015). Convergent evolution of strigolactone perception enabled host detection in parasitic plants. *Science* **349**:540–543.
31. Zhou, F., Lin, Q. and Zhu, L. (2013). D14-SCF(D3)-dependent degradation of D53 regulates strigolactone signalling. *Nature* **504**:406–410.
32. Soundappan, I., Bennett, T. and Morffy, N. (2015). SMAX1-LIKE/D53 Family Members Enable Distinct MAX2-Dependent Responses to Strigolactones and Karrikins in *Arabidopsis*. *Plant Cell* **27**:3143–3159.
33. Wang, L., Wang, B. and Yu, H. (2020). Transcriptional regulation of strigolactone signalling in *Arabidopsis*. *Nature* **583**:277–281.
34. Hu, Q., Liu, H. and He, Y. (2024). Regulatory mechanisms of strigolactone perception in rice. *Cell* **187**:7551–7567.
35. Jiang, L., Liu, X. and Xiong, G. (2013). DWARF 53 acts as a repressor of strigolactone signalling in rice. *Nature* **504**:401–405.
36. Wang, L., Wang, B. and Jiang, L. (2015). Strigolactone Signaling in *Arabidopsis* Regulates Shoot Development by Targeting D53-Like SMXL Repressor Proteins for Ubiquitination and Degradation. *Plant Cell* **27**:3128–3142.
37. Umehara, M., Hanada, A., Yoshida, S. et al. (2008). Inhibition of shoot branching by new terpenoid plant hormones. *Nature* **455**:195–200.
38. Gomez-Roldan, V., Fermas, S., Brewer, P.B. et al. (2008). Strigolactone inhibition of shoot branching. *Nature* **455**:189–194.
39. Vogel, J.T., Walter, M.H., Giavalisco, P. et al. (2010). *SlCCD7* controls strigolactone biosynthesis, shoot branching and mycorrhiza-induced apocarotenoid formation in tomato: *SlCCD7* controls tomato branching. *Plant J.* **61**:300–311.
40. Butt, H., Jamil, M., Wang, J.Y. et al. (2018). Engineering plant architecture via CRISPR/Cas9-mediated alteration of strigolactone biosynthesis. *BMC Plant Biol.* **18**:174.
41. Bari, V.K., Nassar, J.A., Kheredin, S.M. et al. (2019). CRISPR/Cas9-mediated mutagenesis of *CAROTENOID CLEAVAGE DIOXYGENASE 8* in tomato provides resistance against the parasitic weed *Phelipanche aegyptiaca*. *Sci. Rep.* **9**:11438. DOI:https://doi.org/10.1038/s41598-019-47893-z.
42. Chen, J., Zhang, L., Zhu, M. et al. (2018). *Non-dormant Axillary Bud 1* regulates axillary bud outgrowth in sorghum. *J. Integr. Plant Biol.* **60**:938–955. DOI:https://doi.org/10.1111/jipb.12665.
43. Al-Babili, S. and Bouwmeester, H.J. (2015). Strigolactones, a novel carotenoid-derived plant hormone. *Annu. Rev. Plant Biol.* **66**:161–186. DOI:https://doi.org/10.1146/annurev-arplant-043014-114759.
44. Bari, V.K., Nassar, J.A. and Aly, R. (2021). CRISPR/Cas9 mediated mutagenesis of *MORE AXILLARY GROWTH 1* in tomato confers resistance to root parasitic weed *Phelipanche aegyptiaca*. *Sci. Rep.* **11**:3905. DOI:https://doi.org/10.1038/s41598-021-82897-8.
45. Wakabayashi, T., Hamana, M., Mori, A. et al. (2019). Direct conversion of carlactonoic acid to orobanchol by cytochrome P450 *CYP722C* in strigolactone biosynthesis. *Sci. Adv.* **5**:eaax9067. DOI:https://doi.org/10.1126/sciadv.aax9067.
46. Kretzschmar, T., Kohlen, W., Sasse, J. et al. (2012). A petunia ABC protein controls strigolactone-dependent symbiotic signalling and branching. *Nature* **483**:341–344. DOI:https://doi.org/10.1038/nature10873.
47. Sasse, J., Simon, S., Gübeli, C. et al. (2015). Asymmetric Localizations of the ABC Transporter PaPDR1 Trace Paths of Directional Strigolactone Transport. *Curr. Biol.* **25**:647–655. DOI:https://doi.org/10.1016/j.cub.2015.01.015.
48. Banasiak, J., Borghi, L., Stec, N. et al. (2020). The full-size ABCG transporter of Medicago truncatula is involved in strigolactone secretion, affecting arbuscular mycorrhiza. *Front. Plant Sci.* **11**:18. DOI:https://doi.org/10.3389/fpls.2020.00018.
49. Xie, X., Wang, G., Yang, L. et al. (2015). Cloning and characterization of a novel *Nicotiana tabacum* ABC transporter involved in shoot branching. *Physiol. Plant* **153**:299–306. DOI:https://doi.org/10.1111/ppl.12267.

50. Bari, V.K., Nassar, J.A., Meir, A. et al. (2021). Targeted mutagenesis of two homologous ATP-binding cassette subfamily G (ABCG) genes in tomato confers resistance to parasitic weed *Phelipanche aegyptiaca*. *J. Plant Res.* **134**:585–597. DOI:https://doi.org/10.1007/s10265-021-01275-7.
51. Lin, T., Zhu, G., Zhang, J. et al. (2014). Genomic analyses provide insights into the history of tomato breeding. *Nat. Genet.* **46**:1220–1226. DOI:https://doi.org/10.1038/ng.3117.
52. Zhang, S., Yu, H., Wang, K. et al. (2018). Detection of major loci associated with the variation of 18 important agronomic traits between *Solanum pimpinellifolium* and cultivated tomatoes. *Plant J.* **95**:312–323. DOI:https://doi.org/10.1111/tpj.13952.
53. Shi, J., Zhao, B., Zheng, S. et al. (2021). A phosphate starvation response-centered network regulates mycorrhizal symbiosis. *Cell* **184**:5527–5540.e18. DOI:https://doi.org/10.1016/j.cell.2021.09.030.
54. Li, L., Ge, S., He, L. et al. (2024). SlDELLA interacts with SlPIF4 to regulate arbuscular mycorrhizal symbiosis and phosphate uptake in tomato. *Hortic. Res.* **11**:uhae195. DOI:https://doi.org/10.1093/hr/uhae195.
55. Zhu, G., Wang, S., Huang, Z. et al. (2018). Rewiring of the Fruit Metabolome in Tomato Breeding. *Cell* **172**:249–261.e12. DOI:https://doi.org/10.1016/j.cell.2017.12.019.
56. Lai, Y., Zheng, W., Zheng, Y. et al. (2024). Unveiling a novel entry gate: Insect foregut as an alternative infection route for fungal entomopathogens. *Innovation* **5**:100644. DOI:https://doi.org/10.1016/j.xinn.2024.100644.
57. Qin, L., Deng, Y., Zhang, X. et al. (2024). Mechanistic insights into phosphoactivation of SLAC1 in guard cell signaling. *Proc. Natl. Acad. Sci. USA* **121**:e2323040121. DOI:https://doi.org/10.1073/pnas.2323040121.
58. Xin, P., Guo, Q., Li, B. et al. (2020). A Tailored High-Efficiency Sample Pretreatment Method for Simultaneous Quantification of 10 Classes of Known Endogenous Phytohormones. *Plant Commun.* **1**:100047. DOI:https://doi.org/10.1016/j.xplc.2020.100047.
59. Yoo, S.-D., Cho, Y.-H. and Sheen, J. (2007). *Arabidopsis* mesophyll protoplasts: a versatile cell system for transient gene expression analysis. *Nat. Protoc.* **2**:1565–1572. DOI:https://doi.org/10.1038/nprot.2007.199.
60. Hajný, J., Prát, T. Rydza N. et al. (2020). Receptor kinase module targets PIN-dependent auxin transport during canalization. *Science* **370**:550–557. DOI:https://doi.org/10.1126/science.aba3178.
61. Zha, Y., Chen, C., Jiao, Q. et al. (2024). Comprehensive profiling of antibiotic resistance genes in diverse environments and novel function discovery. *Innov. Life* **2**:100054. DOI:https://doi.org/10.59717/j.xinn-life.2024.100054.
62. Wang, X., Liu, Z., Sun, S. et al. (2021). SISTER OF TM3 activates *FRUITFULL1* to regulate inflorescence branching in tomato. *Hortic. Res.* **8**:251. DOI:https://doi.org/10.1038/s41438-021-00677-x.
63. Zhang, Y., Kilambi, H.V., Liu, J. et al. (2021). ABA homeostasis and long-distance translocation are redundantly regulated by ABCG ABA importers. *Sci. Adv.* **7**:eabf6069. DOI:https://doi.org/10.1126/sciadv.abf6069.
64. Yuan, K., Zhang, H., Yu, C. et al. (2023). Low phosphorus promotes NSP1–NSP2 heterodimerization to enhance strigolactone biosynthesis and regulate shoot and root architecture in rice. *Mol. Plant* **16**:1811–1831. DOI:https://doi.org/10.1016/j.molp.2023.09.022.
65. Li, X., Bai, W., Yang, Q. et al. (2024). The extremotolerant desert moss *Syntrichia caninervis* is a promising pioneer plant for colonizing extraterrestrial environments. *Innovation* **5**:100657. DOI:https://doi.org/10.1016/j.xinn.2024.100657.
66. Zhang, Y., Berman, A. and Shani, E. (2023). Plant Hormone Transport and Localization: Signaling Molecules on the Move. *Annu. Rev. Plant Biol.* **74**:453–479. DOI:https://doi.org/10.1146/annurev-arplant-070722-015329.
67. Zhang, Y., Cheng, X., Wang, Y. et al. (2018). The tomato *MAX1* homolog, *SlMAX1*, is involved in the biosynthesis of tomato strigolactones from carlactone. *New Phytol.* **219**:297–309. DOI:https://doi.org/10.1111/nph.15131.
68. Wang, Y., Durairaj, J., Suárez Duran, H.G. et al. (2022). The tomato cytochrome P450 CYP712G1 catalyses the double oxidation of orobanchol *en route* to the rhizosphere signalling strigolactone, solanacol. *New Phytol.* **235**:1884–1899. DOI:https://doi.org/10.1111/nph.18272.
69. Waters, M.T., Gutjahr, C., Bennett, T. et al. (2017). Strigolactone Signaling and Evolution. *Annu. Rev. Plant Biol.* **68**:291–322. DOI:https://doi.org/10.1146/annurev-arplant-042916-040925.
70. Beveridge, C.A., Ross, J.J. and Murfet, I.C. (1994). Branching Mutant *rms-2* in *Pisum sativum* (Grafting Studies and Endogenous Indole-3-Acetic Acid Levels). *Plant Physiol.* **104**:953–959. DOI:https://doi.org/10.1104/pp.104.3.953.
71. Turnbull, C.G., Booker, J.P. and Leyser, H.M. (2002). Micrografting techniques for testing long-distance signalling in *Arabidopsis*. *Plant J.* **32**:255–262. DOI:https://doi.org/10.1046/j.1365-313X.2002.01419.x.
72. Napoli, C. (1996). Highly Branched Phenotype of the Petunia *dad1-1* Mutant Is Reversed by Grafting. *Plant Physiol.* **111**:27–37. DOI:https://doi.org/10.1104/pp.111.1.27.
73. Seto, Y. and Yamaguchi, S. (2014). Strigolactone biosynthesis and perception. *Curr. Opin. Plant Biol.* **21**:1–6. DOI:https://doi.org/10.1016/j.pbi.2014.06.001.
74. Tippe, D.E., Bastiaans, L., van Ast, A. et al. (2020). Fertilisers differentially affect facultative and obligate parasitic weeds of rice and only occasionally improve yields in infested fields. *Field Crops Res.* **254**:107845. DOI:https://doi.org/10.1016/j.fcr.2020.107845.
75. Jamil, M., Charnikhova, T., Cardoso, C. et al. (2011). Quantification of the relationship between strigolactones and *Striga hermonthica* infection in rice under varying levels of nitrogen and phosphorus. *Weed Res.* **51**:373–385. DOI:https://doi.org/10.1111/j.1365-3180.2011.00847.x.
76. Jamil, M., Kanampiu, F.K., Karaya, H. et al. (2012). *Striga hermonthica* parasitism in maize in response to N and P fertilisers. *Field Crops Res.* **134**:1–10. DOI:https://doi.org/10.1016/j.fcr.2012.03.015.
77. Haider, I., Yunmeng, Z., White, F. et al. (2023). Transcriptome analysis of the phosphate starvation response sheds light on strigolactone biosynthesis in rice. *Plant J.* **114**:355–370. DOI:https://doi.org/10.1111/tpj.16140.
78. Liu, W., Kohlen, W., Lillo, A. et al. (2011). Strigolactone Biosynthesis in *Medicago truncatula* and Rice Requires the Symbiotic GRAS-Type Transcription Factors NSP1 and NSP2. *Plant Cell* **23**:3853–3865. DOI:https://doi.org/10.1105/tpc.111.089771.
79. Guillotin, B., Etemadi, M., Audran, C. et al. (2017). *Sl-IAA27* regulates strigolactone biosynthesis and mycorrhization in tomato (var. *MicroTom*). *New Phytol.* **213**:1124–1132. DOI:https://doi.org/10.1111/nph.14246.
80. Ofori, P.A., Mizuno, A., Suzuki, M. et al. (2018). Genome-wide analysis of ATP binding cassette (ABC) transporters in tomato. *PLoS. One* **13**:e0200854. DOI:https://doi.org/10.1371/journal.pone.0200854.
81. Westwood, J.H., Yoder, J.I., Timko, M.P. et al. (2010). The evolution of parasitism in plants. *Trends Plant Sci.* **15**:227–235. DOI:https://doi.org/10.1016/j.tplants.2010.01.004.
82. Xu, Y., Zhang, J., Ma, C. et al. (2022). Comparative genomics of Orobanchaceous species with different parasitic lifestyles reveals the origin and stepwise evolution of plant parasitism. *Mol. Plant* **15**:1384–1399. DOI:https://doi.org/10.1016/j.molp.2022.07.007.
83. Yoshida, S., Kim, S., Wafula, E.K. et al. (2019). Genome Sequence of *Striga asiatica* Provides Insight into the Evolution of Plant Parasitism. *Curr. Biol.* **29**:3041–3052.e4. DOI:https://doi.org/10.1016/j.cub.2019.07.086.
84. Kohlen, W., Charnikhova, T., Lammers, M. et al. (2012). The tomato *CAROTENOID CLEAVAGE DIOXYGENASE8 (SlCCD8)* regulates rhizosphere signaling, plant architecture and affects reproductive development through strigolactone biosynthesis. *New Phytol.* **196**:535–547. DOI:https://doi.org/10.1111/j.1469-8137.2012.04265.x.
85. Wang, Y., Shang, L., Yu, H. et al. (2020). A Strigolactone Biosynthesis Gene Contributed to the Green Revolution in Rice. *Mol. Plant* **13**:923–932. DOI:https://doi.org/10.1016/j.molp.2020.03.009.
86. Ito, S., Braguy, J., Wang, J.Y. et al. (2022). Canonical strigolactones are not the major determinant of tillering but important rhizospheric signals in rice. *Sci. Adv* **8**:eadd1278. DOI:https://doi.org/10.1126/sciadv.add1278.
87. Zhou, Y. and Xu, C. (2023). Miniature genome editors derived from engineering Cas9 ancestor. *Innov. Life* **1**:100008. DOI:https://doi.org/10.59717/j.xinn-life.2023.100008.
88. Duan, Z., Liang, Y., Sun, J. et al. (2024). An engineered Cas12i nuclease that is an efficient genome editing tool in animals and plants. *Innovation* **5**:100564. DOI:https://doi.org/10.1016/j.xinn.2024.100564.

ACKNOWLEDGMENTS

We thank Prof. Jun Zhao from the Inner Mongolia Agricultural University for providing seeds of *O. cumana* race E and F. We thank Shuangyin Zhao, Jie Dong, and Shunli Huo from the Agricultural Science Institute of Bayingolin Mongolian Autonomous Prefecture of Xinjiang, China, for field management. We thank Prof. Jincai Shi from the Nanjing Agricultural University for help in detecting symbiosis with AM fungi. This research was supported by grants from the National Natural Science Foundation of China (32122012, 31788103), CAS Project for Young Scientists in Basic Research (YSBR-078), the Strategic Priority Research Program of Chinese Academy of Sciences (XDB1090201), and the Youth Innovation Promotion Association of the Chinese Academy of Sciences (Y2023025).

AUTHOR CONTRIBUTIONS

B.W., J.L., and X.C. conceived and supervised the study. X.B. performed most experiments. L.Q. and Y.C. contributed to the *Xenopus* oocyte experiment. J.Y., P.X., and J.C. performed SL level analyses. Q.L. and Q.H. helped with GUS staining and biochemical analyses. J.W., Y.H., and Z.Y. helped with generation of transgenic plants. X.S. and T.L. performed GWAS analysis. L.K. performed RNA sequencing analysis. Y.Z., L.D., H.B., H.Y., Q.Y., S.H., Q.X., and X.C. analyzed the data. B.W., X.B., and J.L. wrote the manuscript. All authors have read, edited, and approved the content of the manuscript.

DECLARATION OF INTERESTS

The authors declare no competing interests.

SUPPLEMENTAL INFORMATION

Supplemental information can be found online at https://doi.org/10.1016/j.xinn.2025.100815.

LEAD CONTACT WEBSITE

The lead contact website is http://english.genetics.cas.cn/sourcedb/people/peop/faculty/202311/t20231107_641746.html.